Geometry and dynamics in moduli spaces
Lecture 1. Random hyperbolic surfaces
(Riemann surfaces seen without glasses)

Anton Zorich
Université Paris Cité
March 3, 2026

“There are methods and formulae in science, which serve as master-keys to many apparently different problems. The resources of such things have to be refilled from time to time. In my opinion at the present time we have to develop an art of handling sums over random surfaces.”

A. Polyakov, Quantum geometry of bosonic strings, 1981

(The citation is stolen (with gratitude) from a talk by J. Bouttier)

Hyperbolic word

Random surfaces

We usually draw a hyperbolic surface of large genus g topologically, as a sausage with g holes:

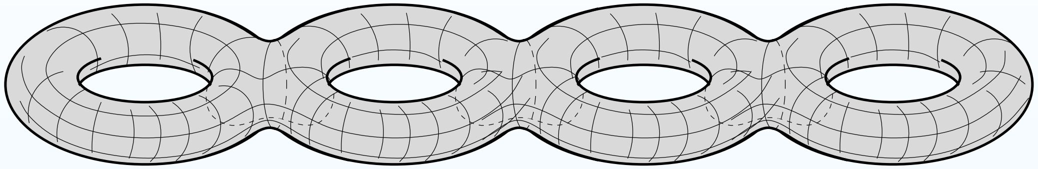

We all know how a random human looks like. Number theorists know how a random integer number looks like. Combinatorists know how a random permutation looks like. A question for geometers: how does a random hyperbolic surface of genus g looks like *when you take your glasses off*?

Random surfaces

We usually draw a hyperbolic surface of large genus g topologically, as a sausage with g holes:

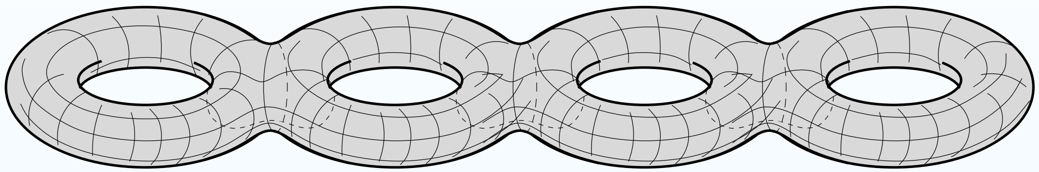

We all know how a random human looks like. Number theorists know how a random integer number looks like. Combinatorists know how a random permutation looks like. A question for geometers: how does a random hyperbolic surface of genus g looks like *when you take your glasses off*?

Following Maryam Mirzakhani's approach, announced in her 2010 ICM talk, by "random" we mean the following. We have a *finite* Weill–Petersson volume form on $\mathcal{M}_{g,n}$. We can normalize it to the probability measure on $\mathcal{M}_{g,n}$. Fix n (for example $n = 0$) and let $g \to \infty$. How does a Weil–Petersson random hyperbolic surface in $\mathcal{M}_{g,n}$ of large genus g and fixed n look like?

Versions of notions of random surfaces emerged independently in quantum gravity, in probability (Gaussian free fields, generalizing Brownian motion to two dimensions), and in combinatorics (random maps and random graphs). All these random surfaces are related.

Portraits of random permutations

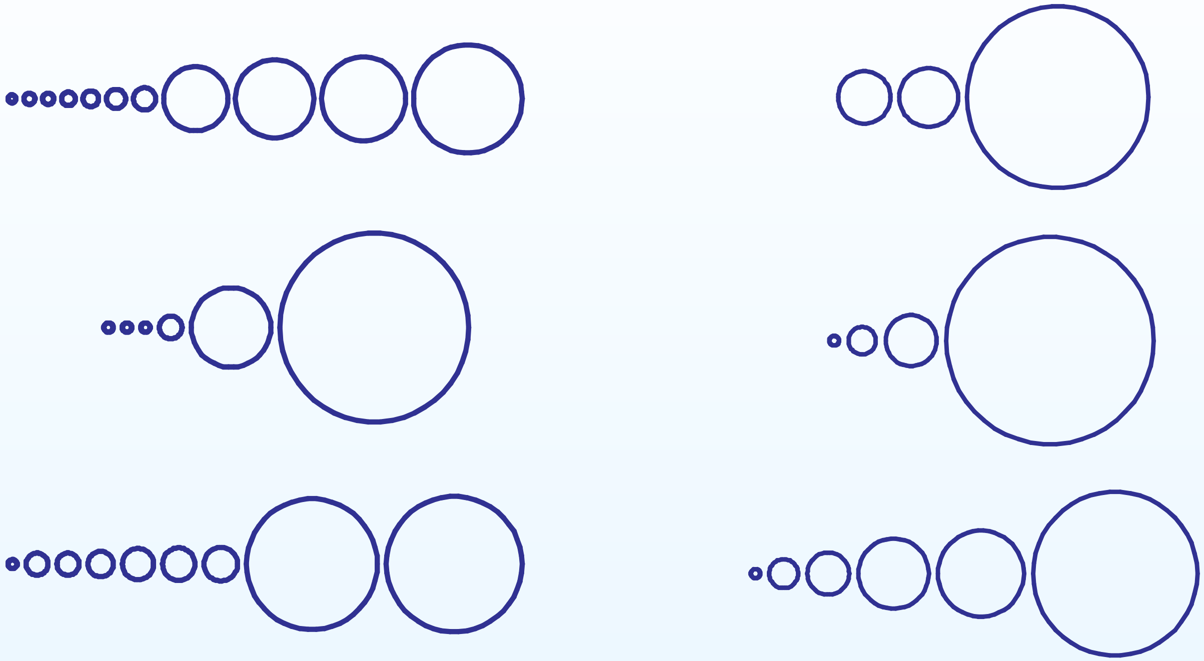

Cycle structure of six random permutations of size 500, where circle areas are drawn in proportion to cycle length. Permutations tend to have a few small cicles, a few large ones, and alltogether have $\sim \log n$ cycles on average.

(Figure III.11 from the book of P. Flajolet and R. Sedgewick “Analytic combinatorics”)

Statistics of prime decompositions: random integer numbers

The Prime Number Theorem states that an integer number n taken randomly in a large interval $[1, N]$ is prime with asymptotic probability $\frac{\log N}{N}$.

One can tell much more about prime decomposition of a large random integer. Denote by $\omega(n)$ the number of prime divisors of an integer n counted without multiplicities. In other words, if n has prime decomposition $n = p_1^{m_1} \dots p_k^{m_k}$, let $\omega(n) = k$. By the Erdős–Kac theorem, the centered and rescaled distribution prescribed by the counting function $\omega(n)$ tends to the normal distribution:

Erdős–Kac Theorem (1939)

$$\lim_{N\to+\infty} \frac{1}{N} \operatorname{card} \left\{ n \le N \,\middle|\, \frac{\omega(n) - \log\log N}{\sqrt{\log\log N}} \le x \right\} = \frac{1}{\sqrt{2\pi}} \int_{-\infty}^{x} e^{-\frac{t^2}{2}}\, dt\,.$$

The subsequent results of A. Selberg (1954) and of A. Rényi and P. Turán (1958) describe the rate of convergence.

Geometric characteristics of a hyperbolic surface

- *Curvature* $= -1$
- $\mathrm{Area}(X) = 2\pi(2g-2)$.
- *Separating systole*:
the shortest *separating* closed geodesic;
its length is denoted by $\ell_{ssys}(X)$
- *Systole*:
the shortest closed geodesic;
its length is denoted by $\ell_{sys}(X)$

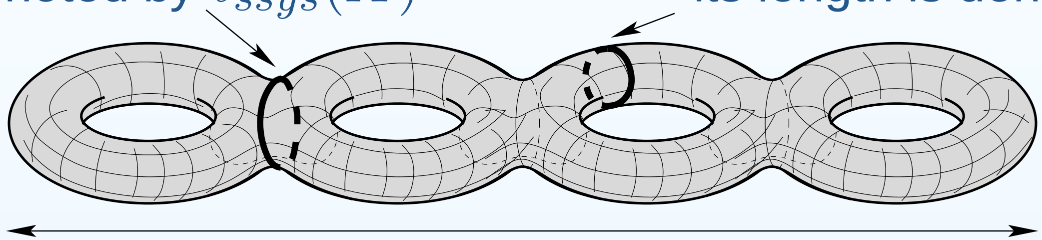

- *Diameter* $\mathrm{diam}(X) = \max_{P_1,P_2 \in X} \mathrm{dist}(P_1, P_2)$
- *Cheeger constant* $h(X)$

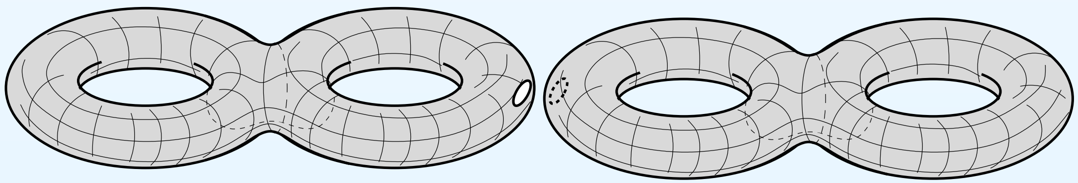

$$h(X) = \inf_{\substack{Y \subset X \\ \mathrm{Area}(Y) \leq \frac{\mathrm{Area}(X)}{2}}} \left(\frac{\ell(\partial Y)}{\mathrm{Area}(Y)} \right).$$

- *First non-zero eigenvalue* $\lambda_1(X)$ (*spectral gap*) of the hyperbolic Laplacian $\Delta(X)$.

Results

For any $\varepsilon > 0$ the quantities $\mathrm{diam}(X)$, $\ell_{ssys}(X)$, $h(X)$, $\lambda_1(X)$ fit the bounds below with probability which tends to 1 as $g \to \infty$:

$$\begin{array}{rcl} \underbrace{\log g}_{area\ bound} < & \mathrm{diam}(X) < & \underbrace{(40+\varepsilon)\log g}_{Mirzakhani'13} \\ \underbrace{(2-\varepsilon)\log g}_{Mirzakhani'13} < & \ell_{ssys}(X) & \\ 0.01 \approx \underbrace{\frac{\log 2}{2\pi + \log 2}}_{Mirzakhani'13} < & h(X) < & \underbrace{1+\varepsilon}_{hyperbolic\ plane} \\ \underbrace{0.0024}_{Mirzakhani'13} < & \lambda_1(X) < & \underbrace{\frac{1}{4}+\varepsilon}_{Huber'74,\ Cheng'75} \end{array}$$

Moreover,

$$\underbrace{\mathbb{E}(\ell_{sys}(X)) \to 1.61\ldots}_{Mirzakhani-Petri'19}$$

Results

For any $\varepsilon > 0$ the quantities $\mathrm{diam}(X)$, $\ell_{ssys}(X)$, $h(X)$, $\lambda_1(X)$ fit the bounds below with probability which tends to 1 as $g \to \infty$:

$$\underset{area\ bound}{\log g} < \mathrm{diam}(X) < \underset{Wu-Xue'22}{(4+\varepsilon)\log g}$$

$$\underset{Mirzakhani'13}{(2-\varepsilon)\log g} < \ell_{ssys}(X) \quad \underset{Nie-Wu-Xue'23}{2\log g}$$

$$0.1 \approx \underset{Mirzakhani'13}{\frac{\log 2}{2\pi + \log 2}} < h(X) < \underset{Budzinski-Curien-Petri'25}{\leq \frac{2}{\pi} \approx 0.63}$$

$$\underset{\substack{Wu-Xue'23\\ Lipnowski-Wright'23}}{\frac{3}{16}} < \lambda_1(X) < \underset{Huber'74,\ Cheng'75}{\frac{1}{4}+\varepsilon}$$

Moreover,

$$\underset{Mirzakhani-Petri'19}{\mathbb{E}(\ell_{sys}(X)) \to 1.61...}$$

Results

For any $\varepsilon > 0$ the quantities $\operatorname{diam}(X)$, $\ell_{ssys}(X)$, $h(X)$, $\lambda_1(X)$ fit the bounds below with probability which tends to 1 as $g \to \infty$:

$$\underbrace{\log g}_{area\ bound} < \operatorname{diam}(X) < \underbrace{(2+\varepsilon)\log g}_{\substack{from\ \lambda_1 \sim \frac{1}{4} \\ using\ technique\ of\ Magee}}$$

$$\underbrace{(2-\varepsilon)\log g}_{Mirzakhani'13} < \ell_{ssys}(X) \quad \underbrace{2\log g}_{Nie-Wu-Xue'23}$$

$$0.01 \approx \underbrace{\frac{\log 2}{2\pi + \log 2}}_{Mirzakhani'13} < h(X) < \underbrace{\leq \frac{2}{\pi} \approx 0.63}_{Budzinski-Curien-Petri'25}$$

$$\underbrace{\frac{1}{4} - \varepsilon}_{\substack{Anantharaman-Monk'25 \\ Hide-Macera-Thomas'25}} < \lambda_1(X) < \underbrace{\frac{1}{4} + \varepsilon}_{Huber'74,\ Cheng'75}$$

Moreover,

$$\underbrace{\mathbb{E}(\ell_{sys}(X)) \to 1.61\ldots}_{Mirzakhani-Petri'19}$$

Some further results

$$\lim_{g\to\infty} \mathbb{E}\left(\frac{\ell_{ssys}(X)}{\log g}\right) \to \underset{Parlier-Wu-Xu'22}{2}$$

$$\lim_{g\to\infty} \mathbb{E}(\ell_{sys}(X)) \to \underset{Mirzakhani-Petri'19}{1.61..}$$

$$\lim_{g\to\infty} \inf_{X\in\mathcal{M}_g} \frac{\mathrm{diam}(X)}{\log g} \to \underset{Budzinski-Curien-Petri'21}{1}$$

$$\limsup_{g\to\infty} \sup_{X\in\mathcal{M}_g} h(X) \underset{Budzinski-Curien-Petri'25}{\leq \frac{2}{\pi} \approx 0.63}$$

$$\limsup_{g\to\infty} \max_{X\in\mathcal{M}_g} \lambda_1(X) \underset{Huber'74,\ Cheng'75}{\leq \frac{1}{4}}$$

Flat World. Warmup: Average diameter of flat tori

Diameter of a flat torus

Identify the two boundary components of a flat cylinder of perimeter $2\,000\,000$ and of height $\frac{1}{2\,000\,000}$ by an isometry. What diameter has the resulting flat torus?

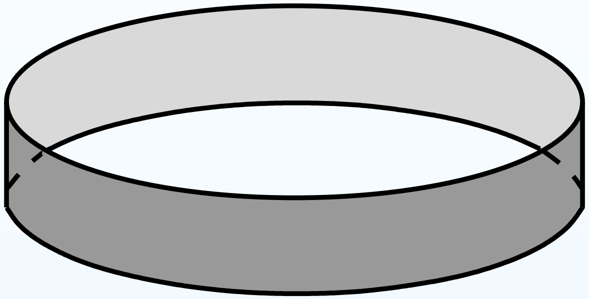

Diameter of a flat torus

Identify the two boundary components of a flat cylinder of perimeter $2\,000\,000$ and of height $\frac{1}{2\,000\,000}$ by an isometry. What diameter has the resulting flat torus?

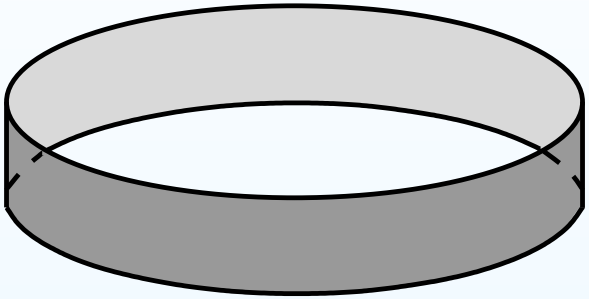

The answer depends on the twist which we apply while gluing the boundary components and might vary from about $1\,000\,000$ to about $\frac{\sqrt{3}}{3} \approx 0.57735$.
Does the average diameter converge when we make cylinders wider?

Any flat torus is a quotient of $\mathbb{R}^2$ by a lattice. It is much easier to compute the diameter of the torus if the lattice is chosen conveniently. The space of lattices up to rotation and under normalization of the shortest lattice vector to length 1 is represented by the modular surface. Let us compute the diameter of a torus defined by a parallelogram with three vertices having coordinates $(0, 0)$, $(1, 0)$, and (x, y) where $0 \leq x \leq \frac{1}{2}$, and $y > 0$ satisfies $x^2 + y^2 \geq 1$ (i.e. the point (x, y) belongs to the modular surface).

Diameter of a flat torus: Voronoï partition

Lemma *Consider a torus given by coordinates* (x, y) *in the fundamental domain. Its diameter is realized on a pair of points, one of which is the origin, and the other — the center of the circle superscribed the triangle with vertices* $(0,0), (1,0), (|x|, y)$*. Diameter* $\operatorname{diam}(T)$ *of the torus* T *proportionally rescaled to have area* 1 *equals*

$$\operatorname{diam}(T) = \frac{\frac{1}{2}\sqrt{1 + \left(y - \frac{|x|(1-|x|)}{y}\right)^2}}{\sqrt{y}}.$$

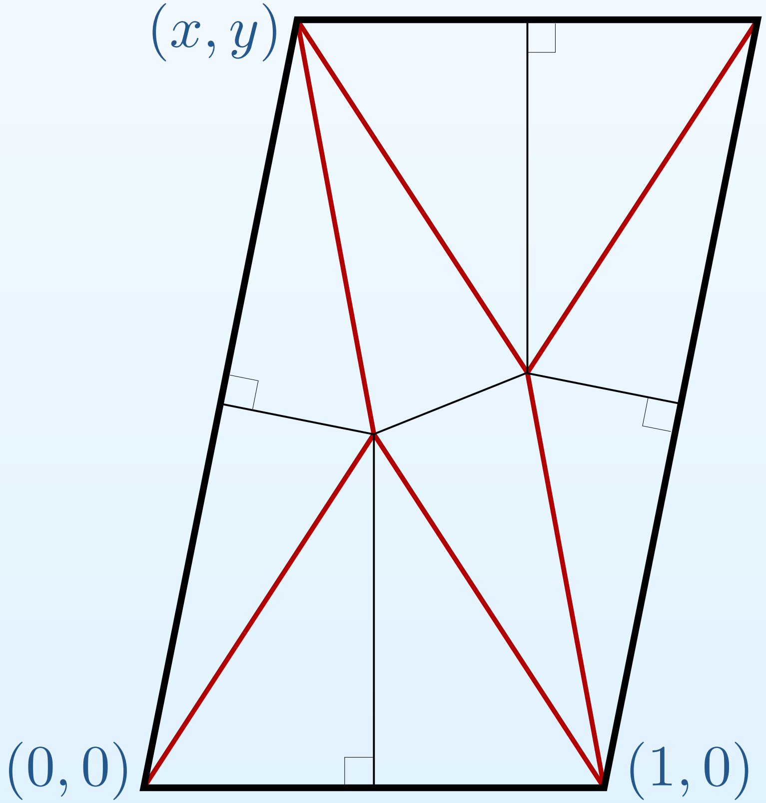

Average diameter of flat tori

Proposition *The average diameter of flat tori of unit area equals*

$$\mathbb{E}(\mathrm{diam}(T)) = \frac{3}{\pi} \int_0^{\frac{1}{2}} \int_{\sqrt{1-x^2}}^{+\infty} \left(\frac{y^2 + \left(y^2 - x(1-x)\right)^2}{y^7} \right)^{\frac{1}{2}} dx\, dy \approx 1.04347\,.$$

Proof. The measure on the modular surface is induced by the hyperbolic metric in the upper half-plane and is given by $\frac{dx\,dy}{y^2}$. The total area of the modular surface is $\frac{\pi}{3}$. The expression for the diameter is symmetric with respect to the change of sign of x, so we can integrate only over the intersection of the modular surface with the positive quadrant. This compensates the factor $\frac{1}{2}$ in the expression for the diameter.

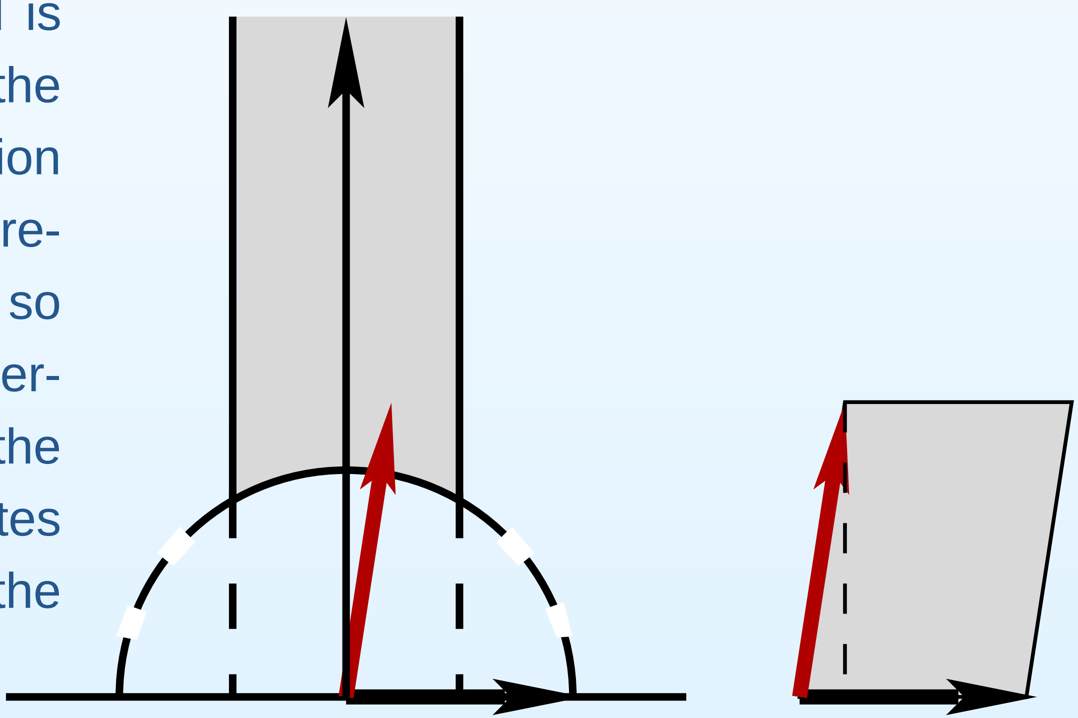

Very flat surfaces

Very flat surface of genus 2

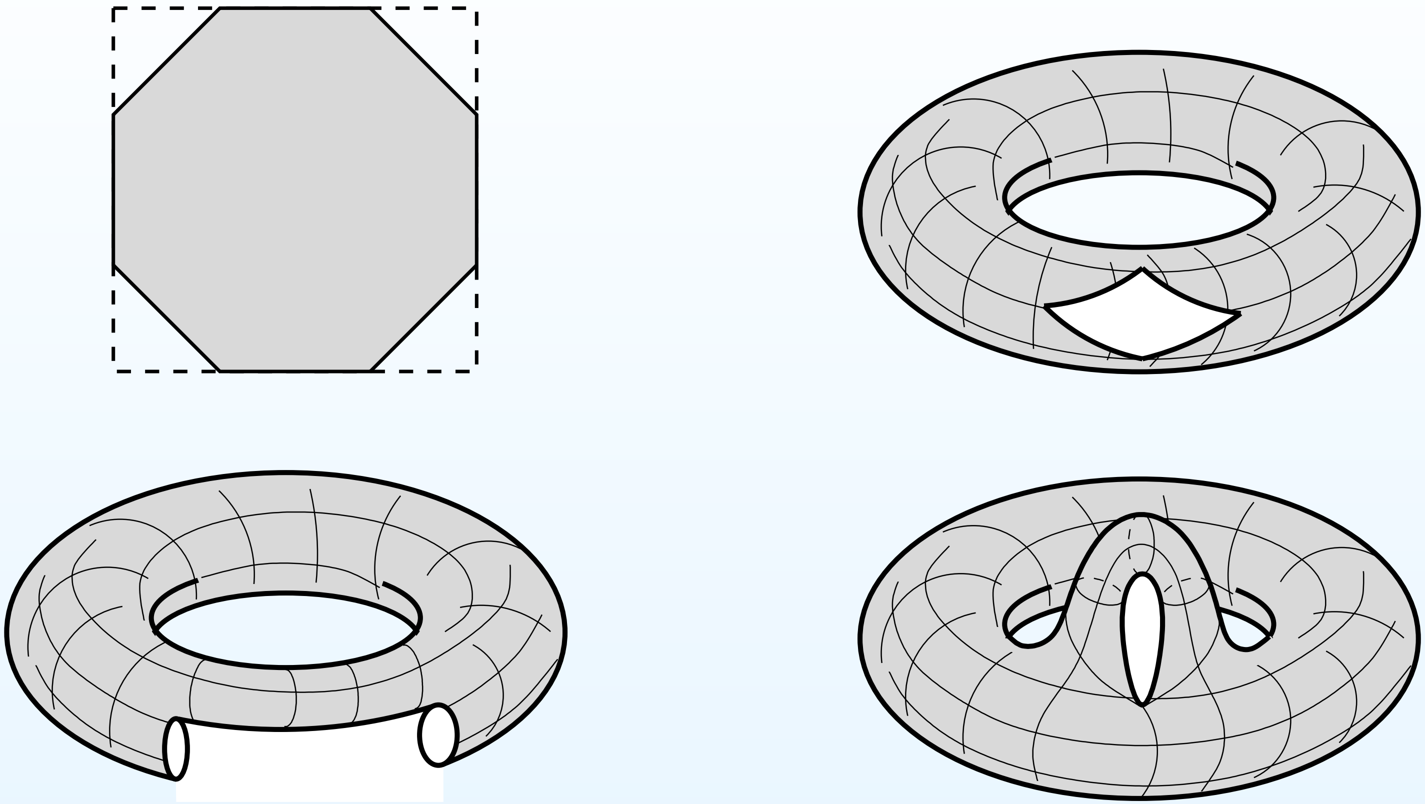

Identifying the opposite sides of a regular octagon we get a flat surface of genus two. All the vertices of the octagon are identified into a single conical singularity. We always consider such a flat surface endowed with a distinguished (say, vertical) direction. By construction, the holonomy of the flat metric is trivial (as for a flat torus).

Very flat surfaces: construction from a polygon

Consider a broken line constructed from vectors $\vec{v}_1, \ldots, \vec{v}_k$.

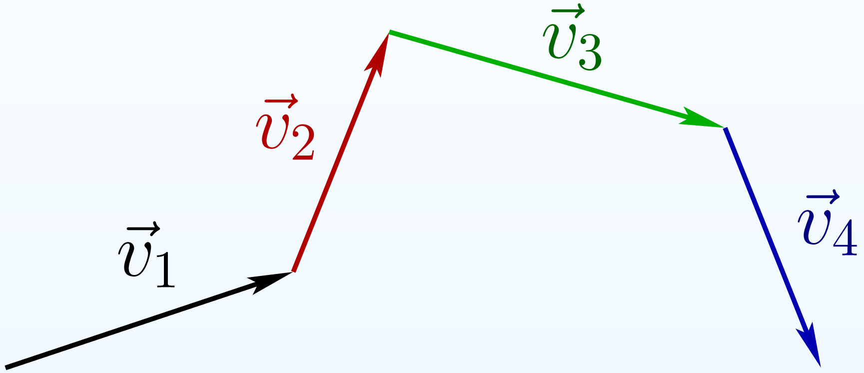

Very flat surfaces: construction from a polygon

Consider a broken line constructed from vectors $\vec{v}_1, \ldots, \vec{v}_k$.

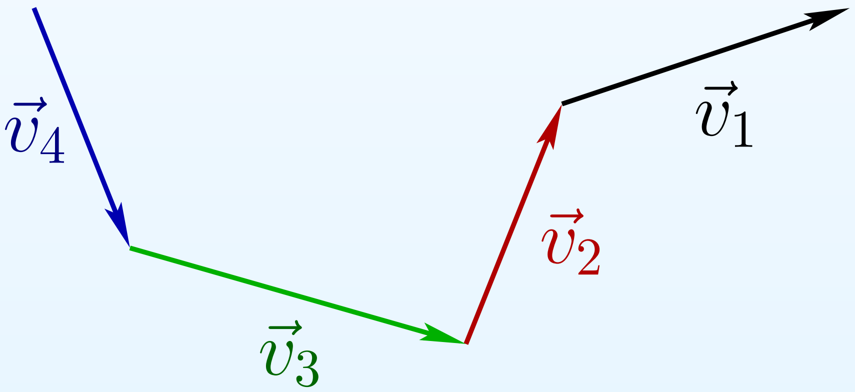

and another one constructed from the same vectors taken in another order.

Very flat surfaces: construction from a polygon

Consider a broken line constructed from vectors $\vec{v}_1, \ldots, \vec{v}_k$.

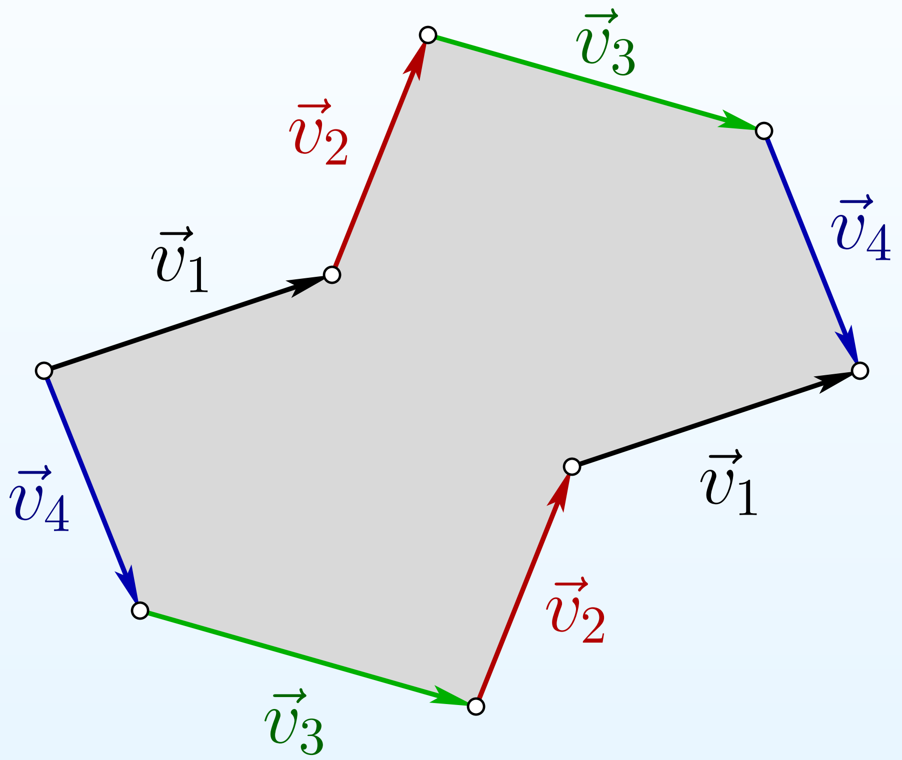

If we are lucky enough the two broken lines do not intersect and form a polygon.

Very flat surfaces: construction from a polygon

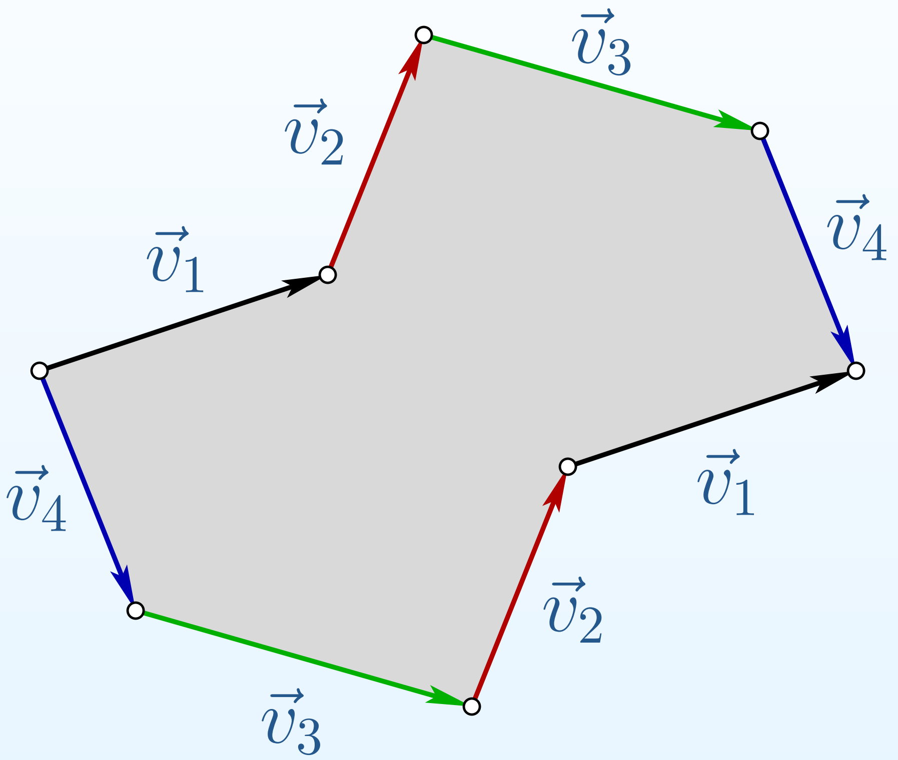

Identifying the corresponding pairs of sides by parallel translations we get a closed surface endowed with a flat metric.

Properties of very flat surfaces

- The flat metric is nonsingular outside of a finite number of conical singularities (inherited from the vertices of the polygon).
- The flat metric has trivial holonomy, i.e. parallel transport along any closed path brings a tangent vector to itself.
- In particular, all cone angles are integer multiples of 2π.
- By convention, the choice of the vertical direction (“direction to the North”) will be considered as a part of the “very flat structure”. For example, a surface obtained from a rotated polygon is considered as a different very flat surface.
- A conical singularity with the cone angle $2\pi \cdot N$ has N outgoing directions to the North.

Flat versus very flat surfaces

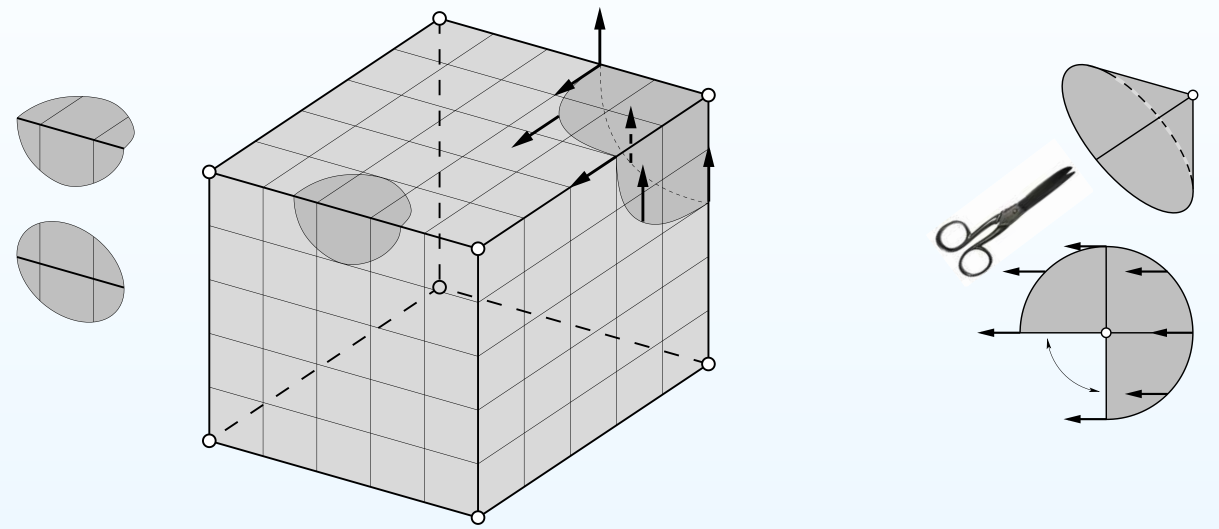

The surface of a cube represents a flat sphere with eight conical singularities. The metric *does not* have singularities on the edges. After parallel transport around a conical singularity a vector comes back pointing to a direction different from the initial one, so this flat metric has *nontrivial holonomy*. The nontrivial holonomy allows, in particular, to generic geodesics to have self-intersections.

Conical singularities

Locally a neighborhood of a conical point looks like a "*monkey saddle*".

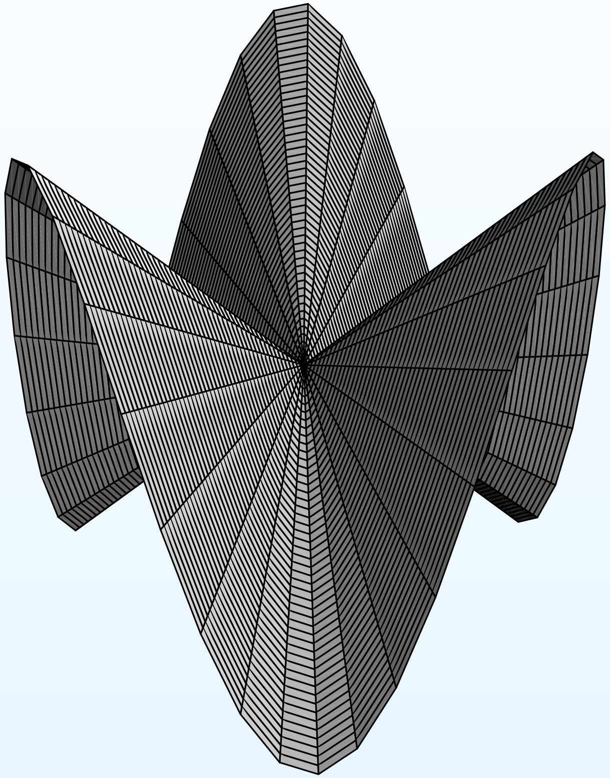

A neighborhood of a conical point with a cone angle 6π can be glued from six metric half discs. At this conical point we have 3 distinct directions to the North.

Families of flat surfaces

The polygon in our construction depends continuously on the vectors $\vec{v}_j$. This means that the combinatorial geometry of the resulting flat surface (its genus g, the number n and types $2\pi(d_1+1), \dots, 2\pi(d_n+1)$ of the resulting conical singularities) does not change under small deformations of the vectors $\vec{v}_j$. This allows to consider a flat surface as an element of a **family** of flat surfaces sharing common combinatorial geometry.

Families of flat surfaces

The polygon in our construction depends continuously on the vectors $\vec{v}_j$. This means that the combinatorial geometry of the resulting flat surface (its genus g, the number n and types $2\pi(d_1+1), \dots, 2\pi(d_n+1)$ of the resulting conical singularities) does not change under small deformations of the vectors $\vec{v}_j$. This allows to consider a flat surface as an element of a **family** of flat surfaces sharing common combinatorial geometry.

As an example of such family one can consider a family of flat tori of area one, which can be identified with the space of lattices of area one:

$$\left.\mathrm{SO}(2,\mathbb{R})\middle\backslash\, \mathrm{SL}(2,\mathbb{R}) \,\middle/\, \mathrm{SL}(2,\mathbb{Z})\right. \quad = \quad \left.\mathbb{H}^2 \middle/ \mathrm{SL}(2,\mathbb{Z})\right.$$

Space of lattices

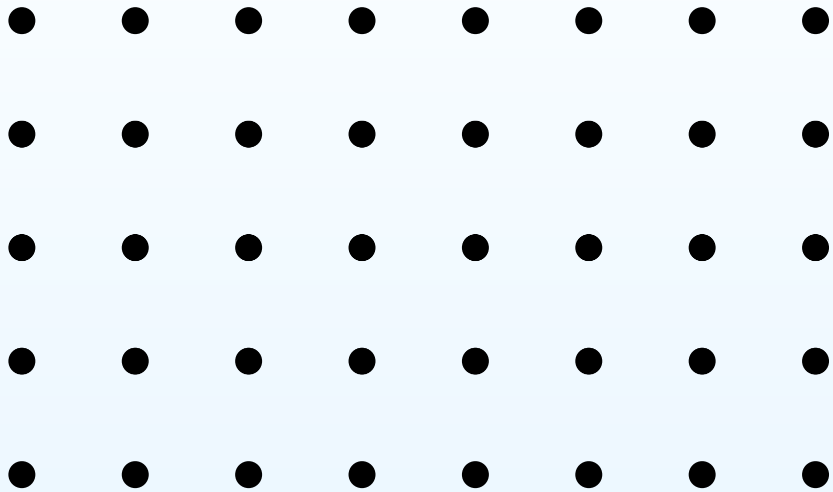

Instead of a single lattice consider a family of all lattices. We can continiously deform a lattice.

Space of lattices

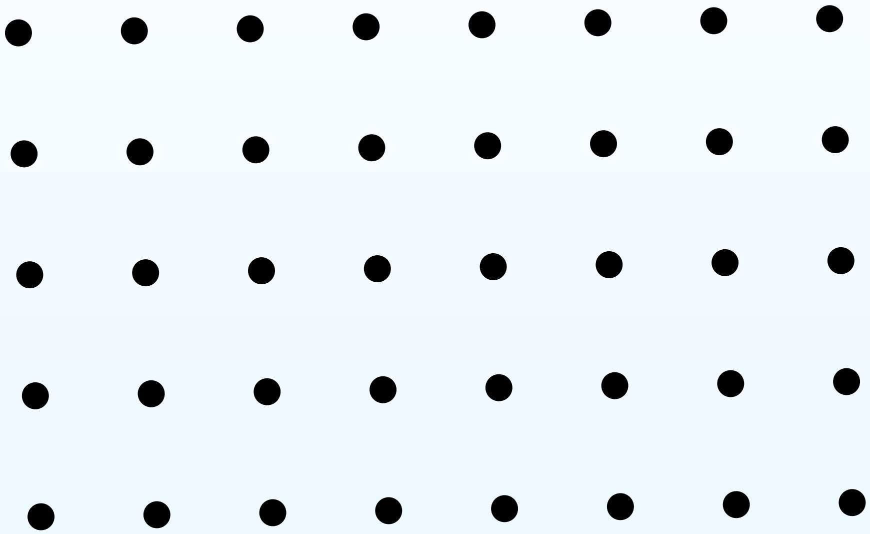

Instead of a single lattice consider a family of all lattices. We can continiously deform a lattice.

Space of lattices

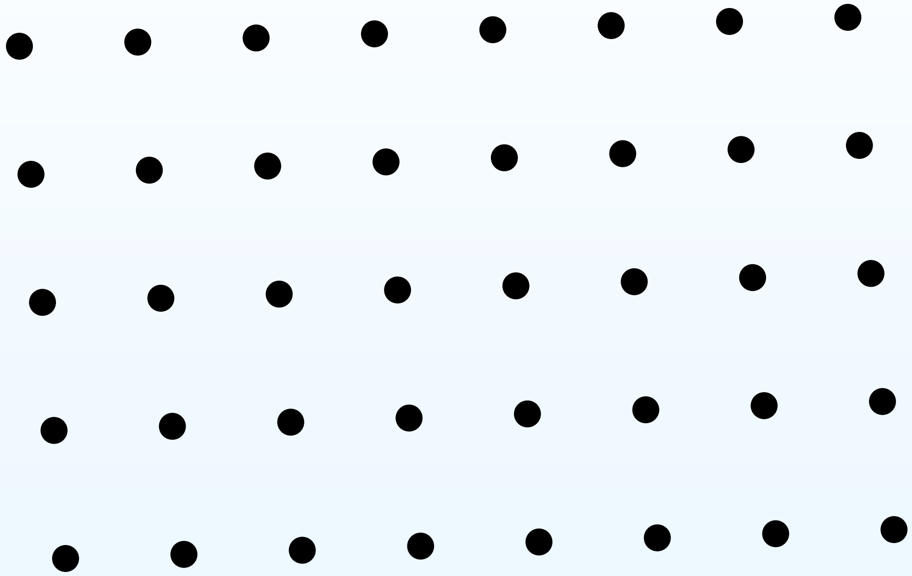

Instead of a single lattice consider a family of all lattices. We can continiously deform a lattice.

Space of lattices

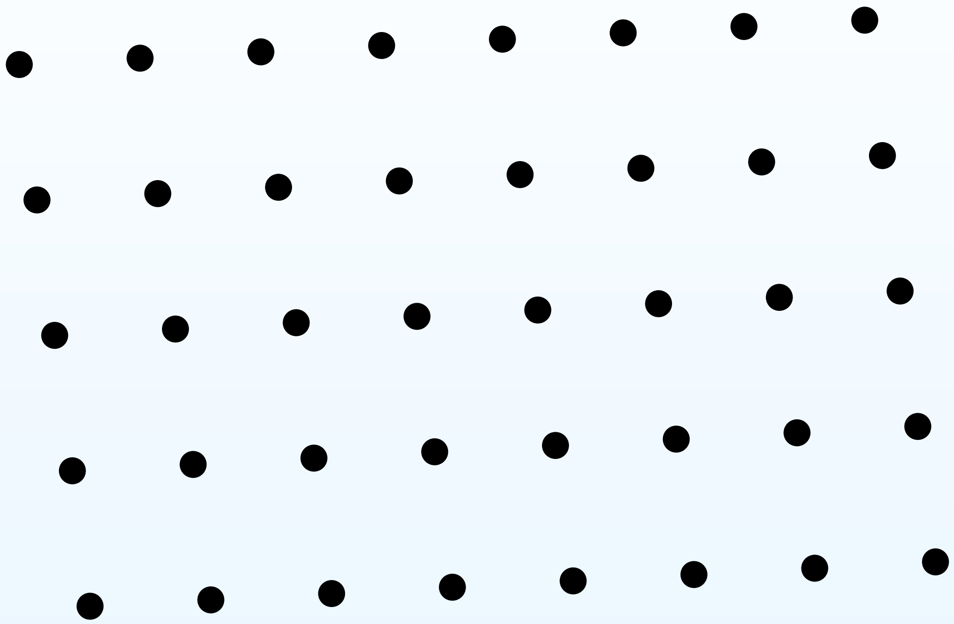

Instead of a single lattice consider a family of all lattices. We can continiously deform a lattice.

Space of lattices

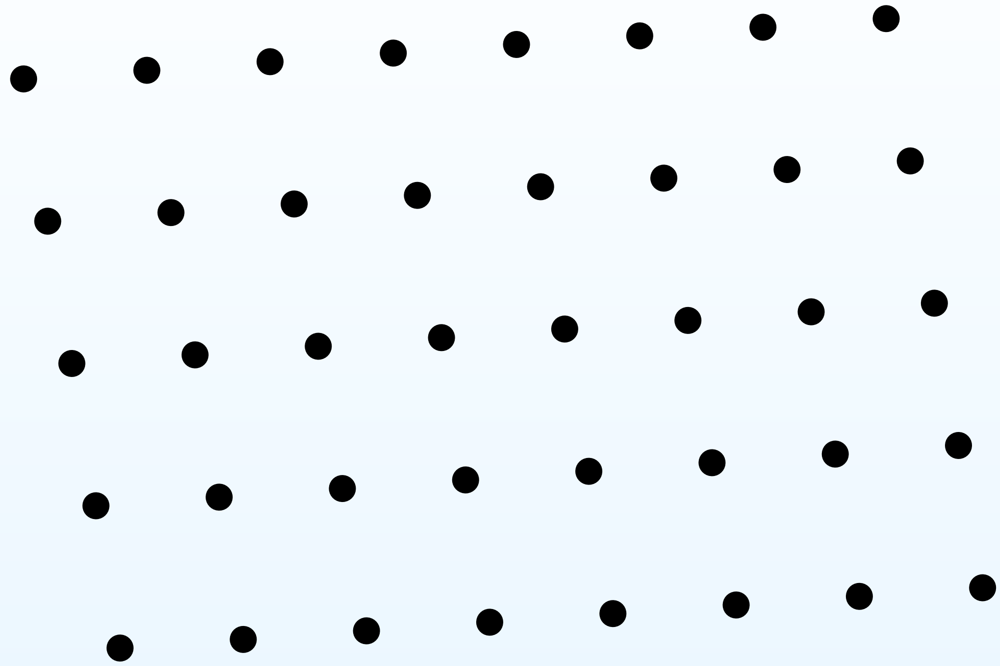

Instead of a single lattice consider a family of all lattices. We can continiously deform a lattice.

Space of lattices

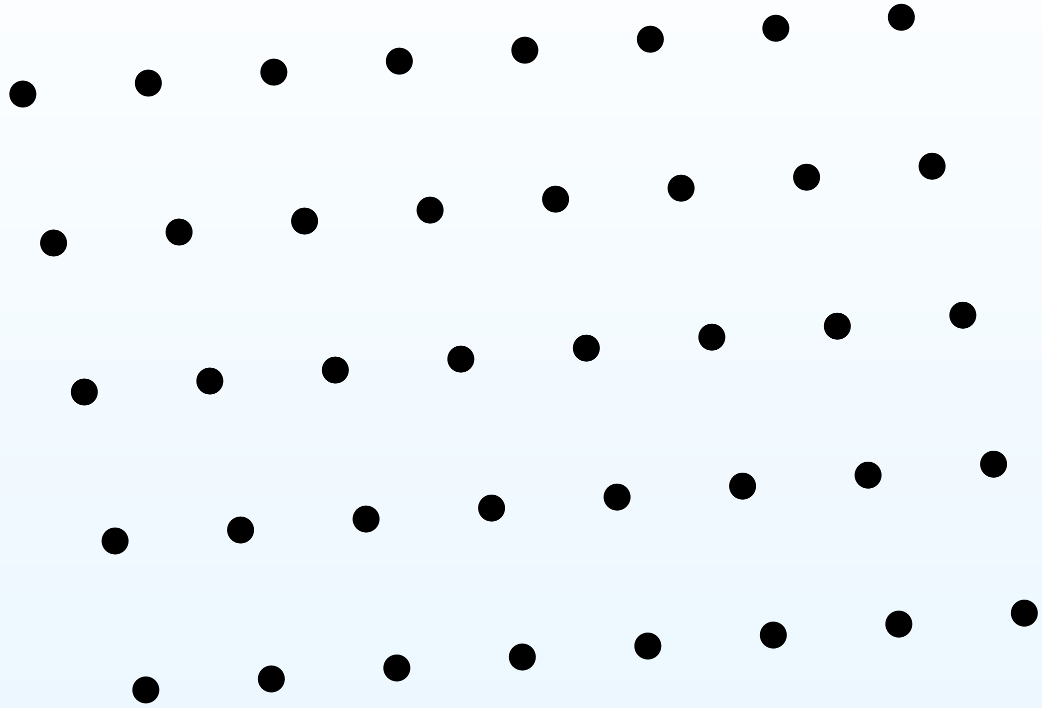

Instead of a single lattice consider a family of all lattices. We can continiously deform a lattice.

Space of lattices

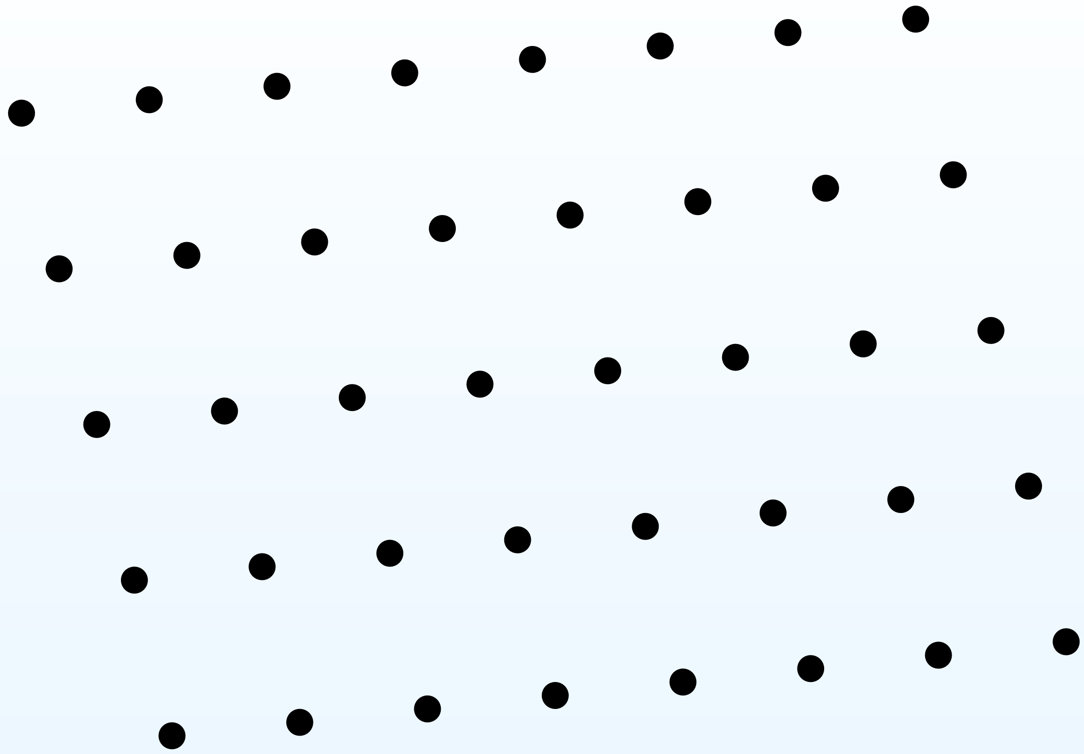

Instead of a single lattice consider a family of all lattices. We can continiously deform a lattice.

Space of lattices

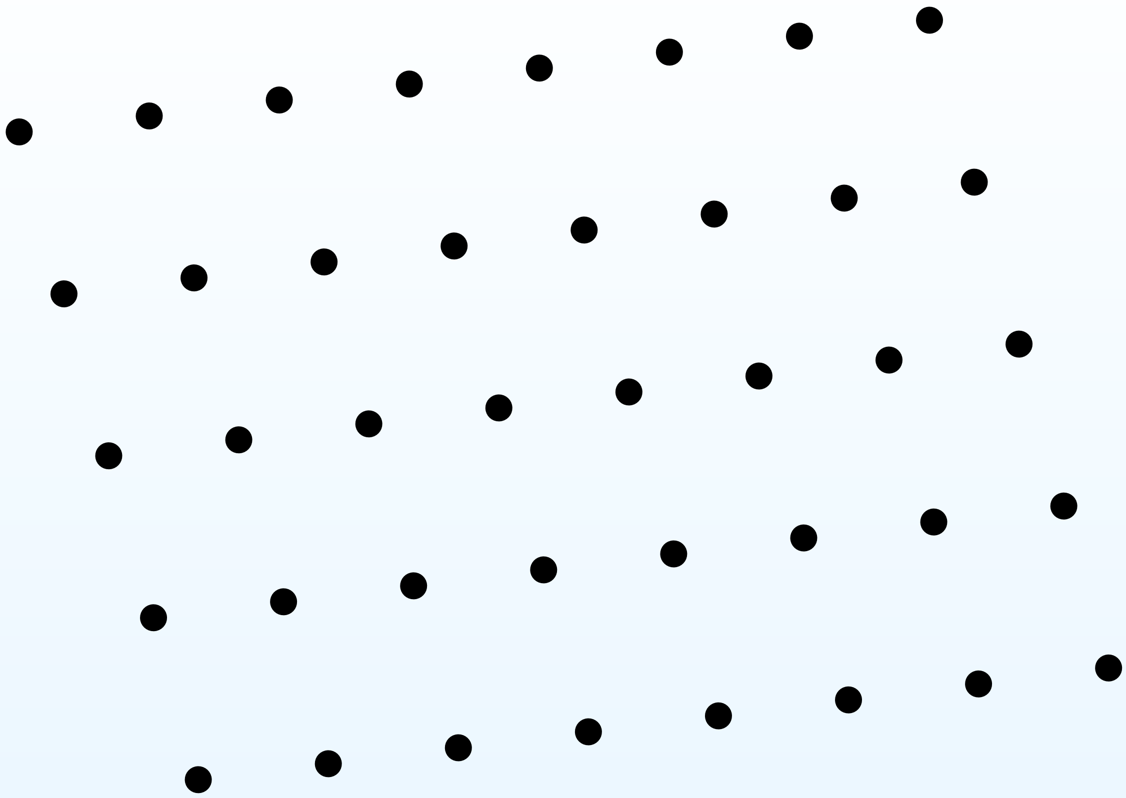

Instead of a single lattice consider a family of all lattices. We can continiously deform a lattice.

Space of lattices

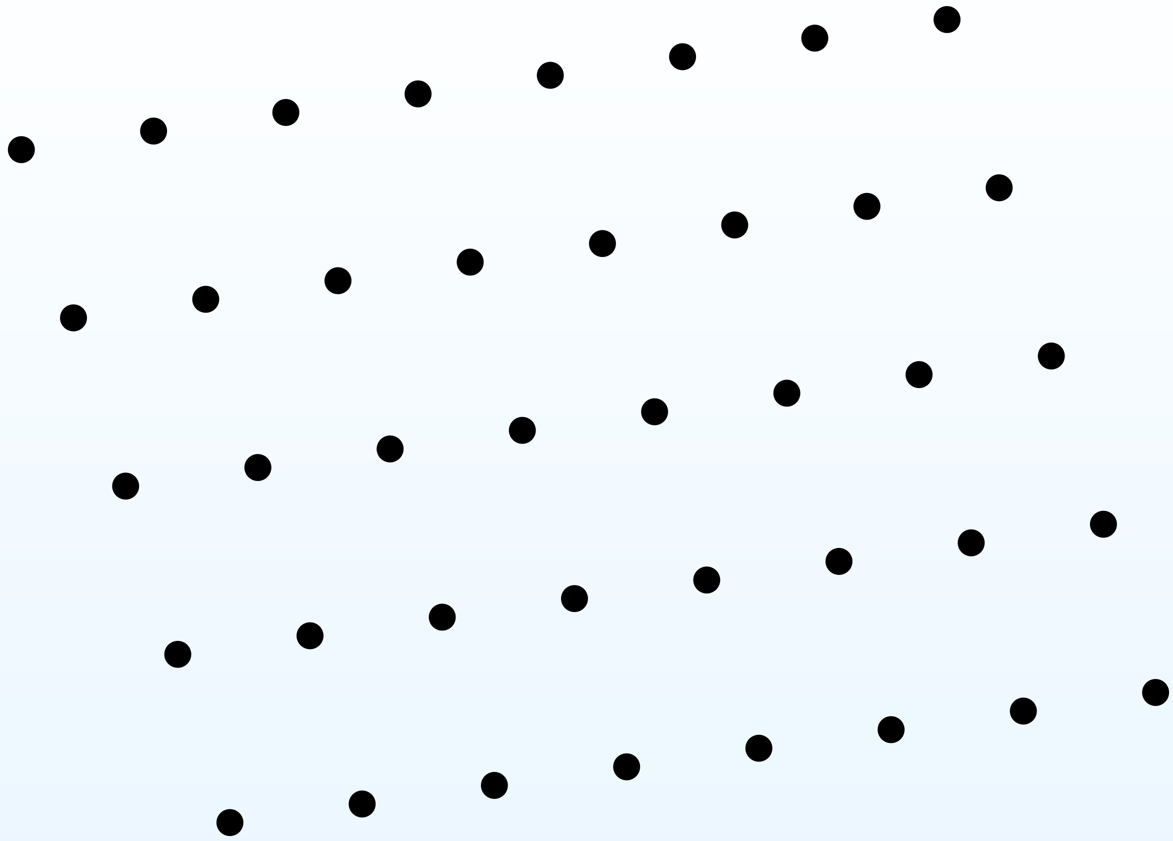

Instead of a single lattice consider a family of all lattices. We can continiously deform a lattice.

Space of lattices

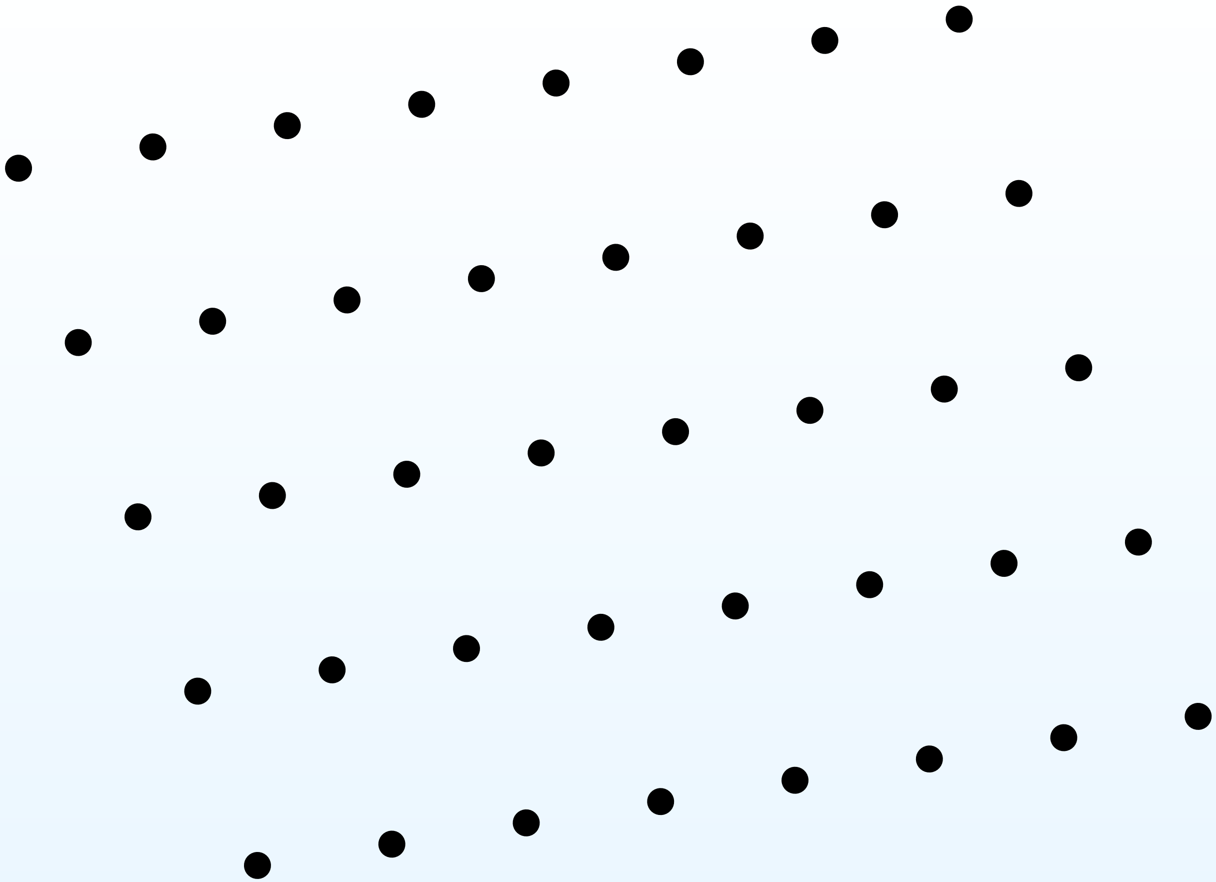

Instead of a single lattice consider a family of all lattices. We can continiously deform a lattice.

Space of lattices

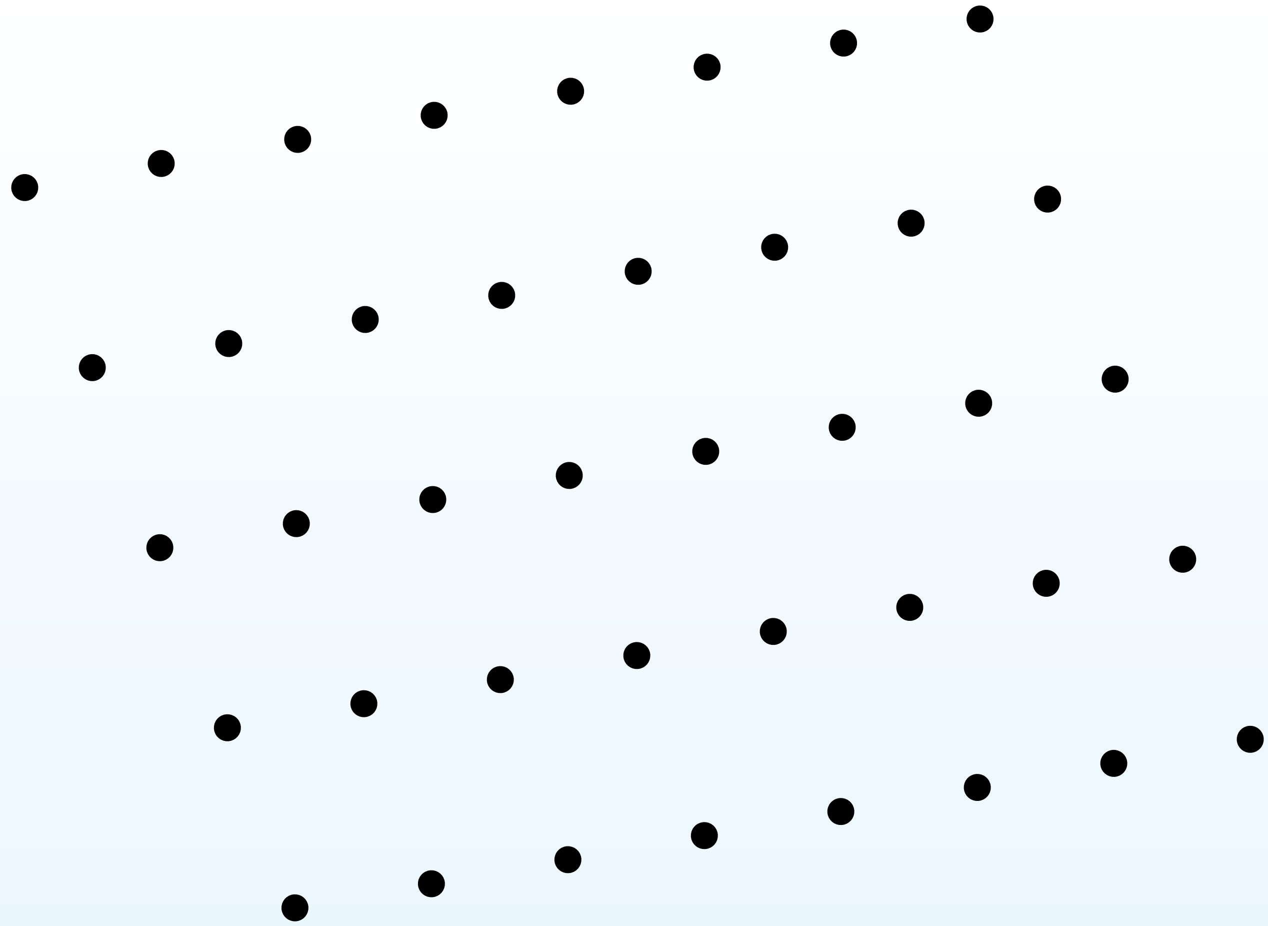

Instead of a single lattice consider a family of all lattices. We can continiously deform a lattice.

If we are interested only by the straight lines (geodesics) on the corresponding flat tori, we do not distinguish lattices which differ by a rotation or a homothety.

Space of lattices

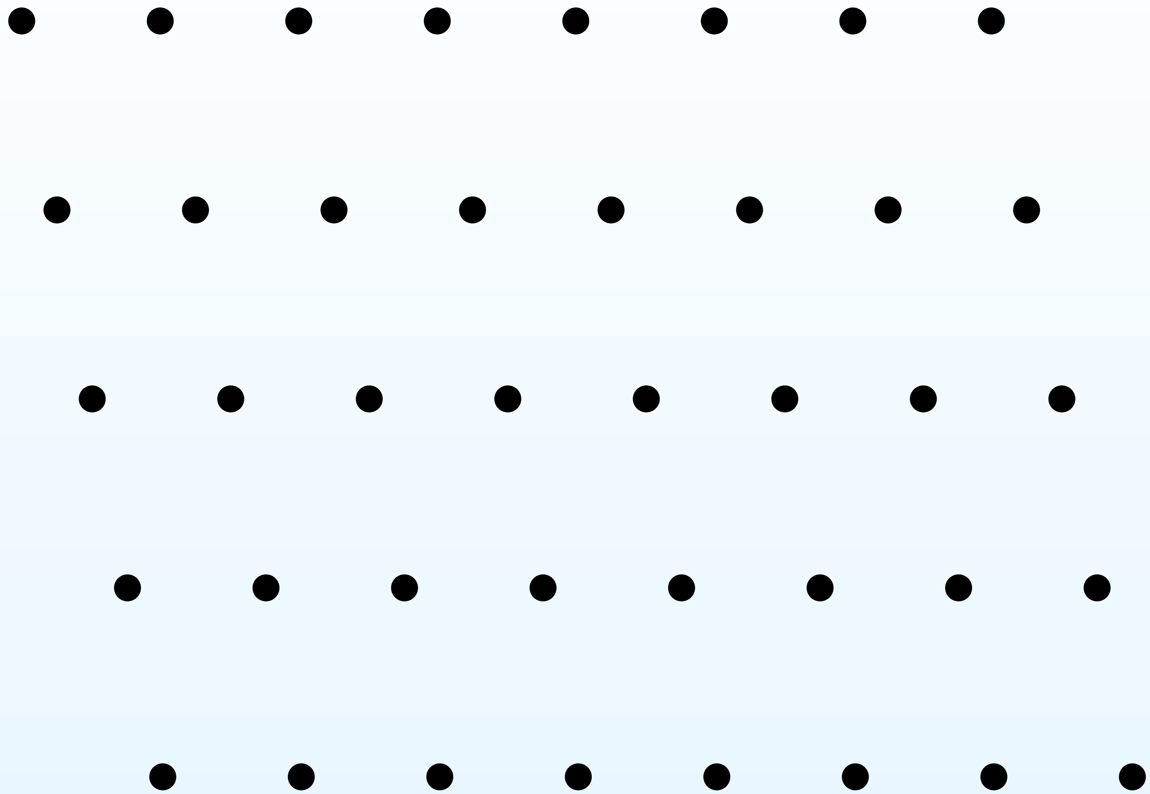

Instead of a single lattice consider a family of all lattices. We can continiously deform a lattice.

If we are interested only by the straight lines (geodesics) on the corresponding flat tori, we do not distinguish lattices which differ by a rotation or a homothety.

Space of lattices

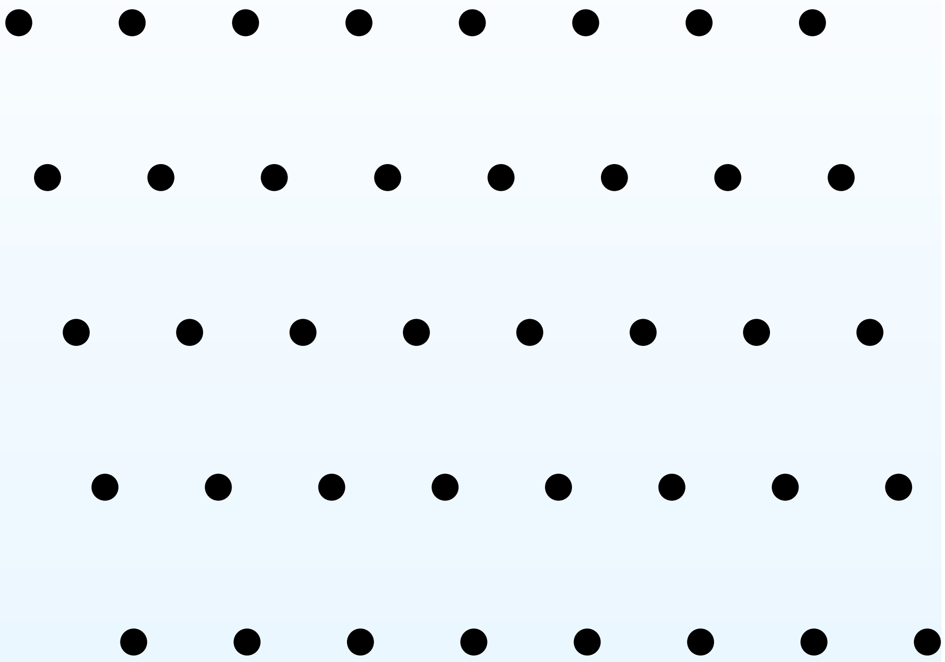

If we are interested only by the straight lines (geodesics) on the corresponding flat tori, we do not distinguish lattices which differ by a rotation or a homothety.

Space of lattices: fundamental domain

- Choosing an appropriate homothety and rotation we can place the shortest vector of the lattice to the horizontal unit vector.

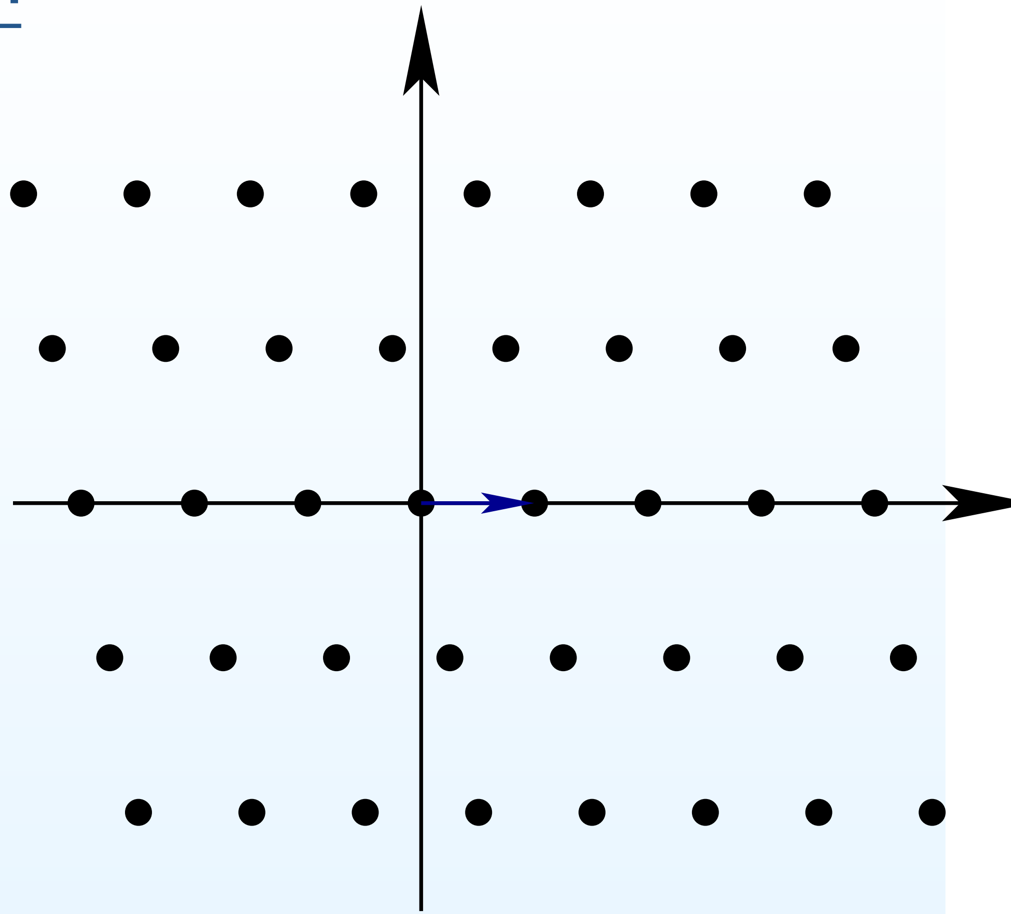

Space of lattices: fundamental domain

- Choosing an appropriate homothety and rotation we can place the shortest vector of the lattice to the horizontal unit vector.
- Consider the shortest vector of the lattice located in the upper half-plane.

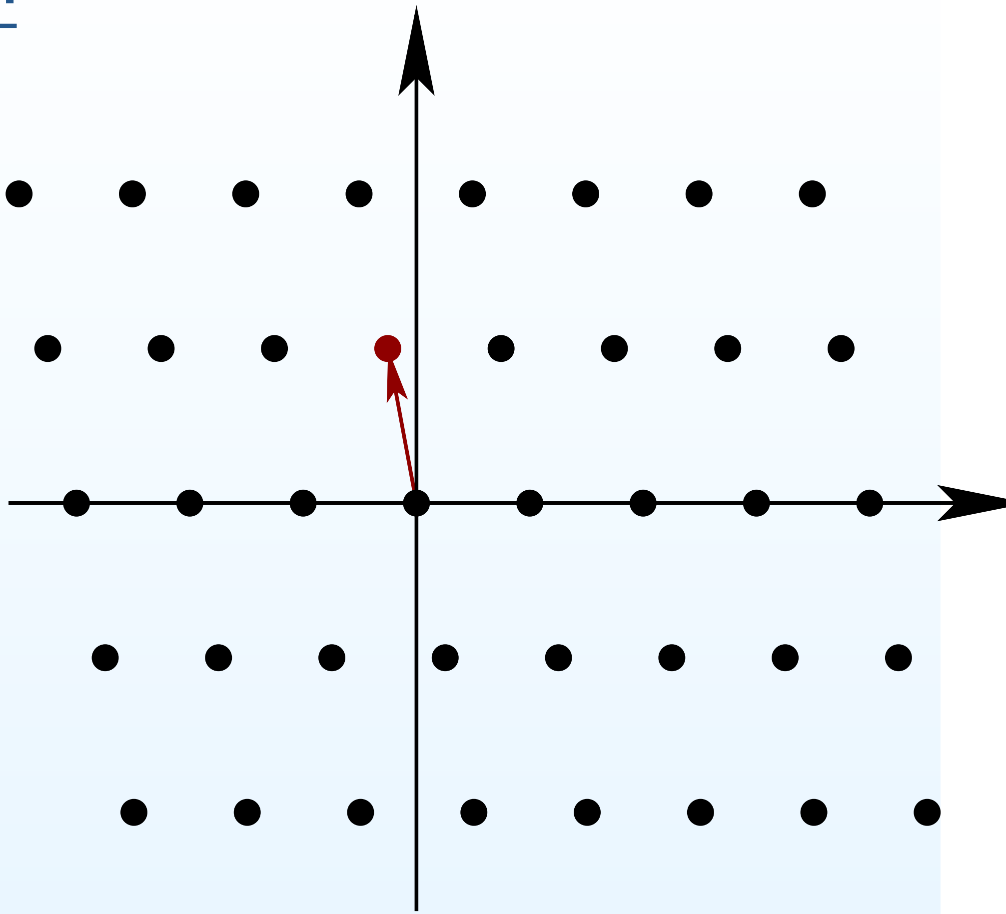

Space of lattices: fundamental domain

- Choosing an appropriate homothety and rotation we can place the shortest vector of the lattice to the horizontal unit vector.
- Consider the shortest vector of the lattice located in the upper half-plane.
- It lives outside the unit disc.

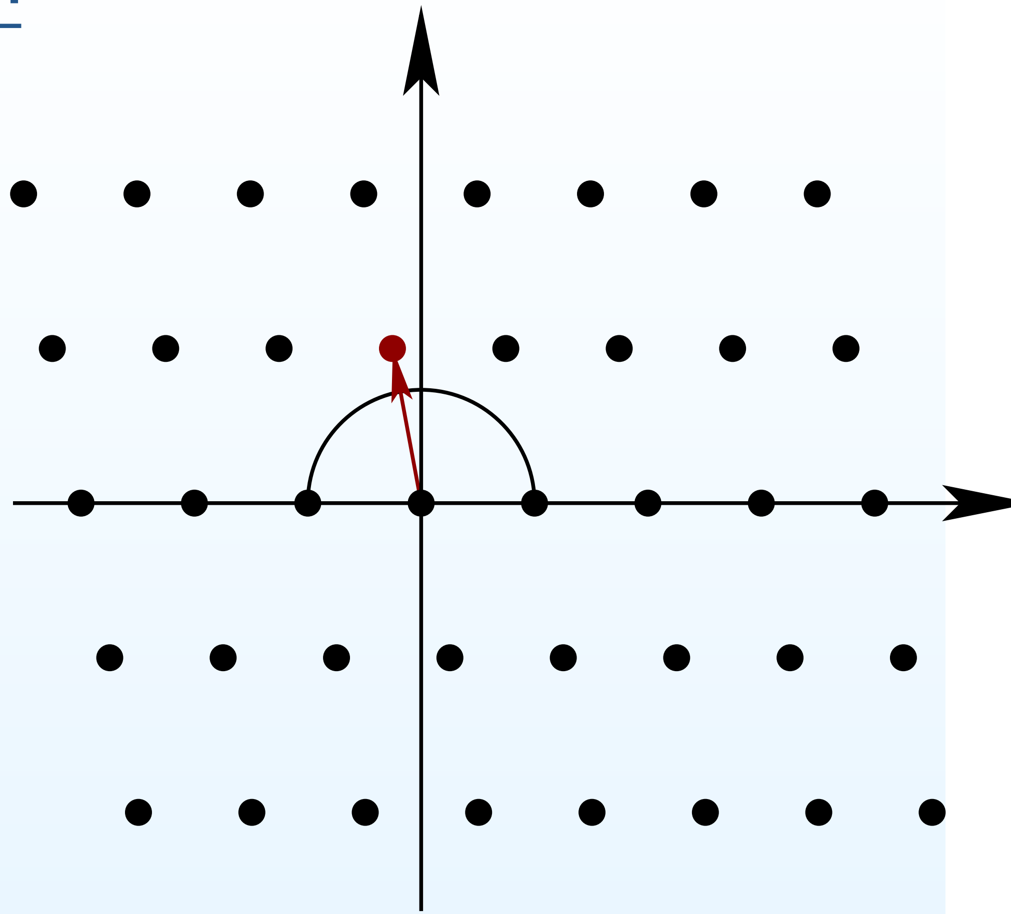

Space of lattices: fundamental domain

- Choosing an appropriate homothety and rotation we can place the shortest vector of the lattice to the horizontal unit vector.
- Consider the shortest vector of the lattice located in the upper half-plane.
- It lives outside the unit disc.
- It belongs to the strip $-1/2 \leq x \leq 1/2$.

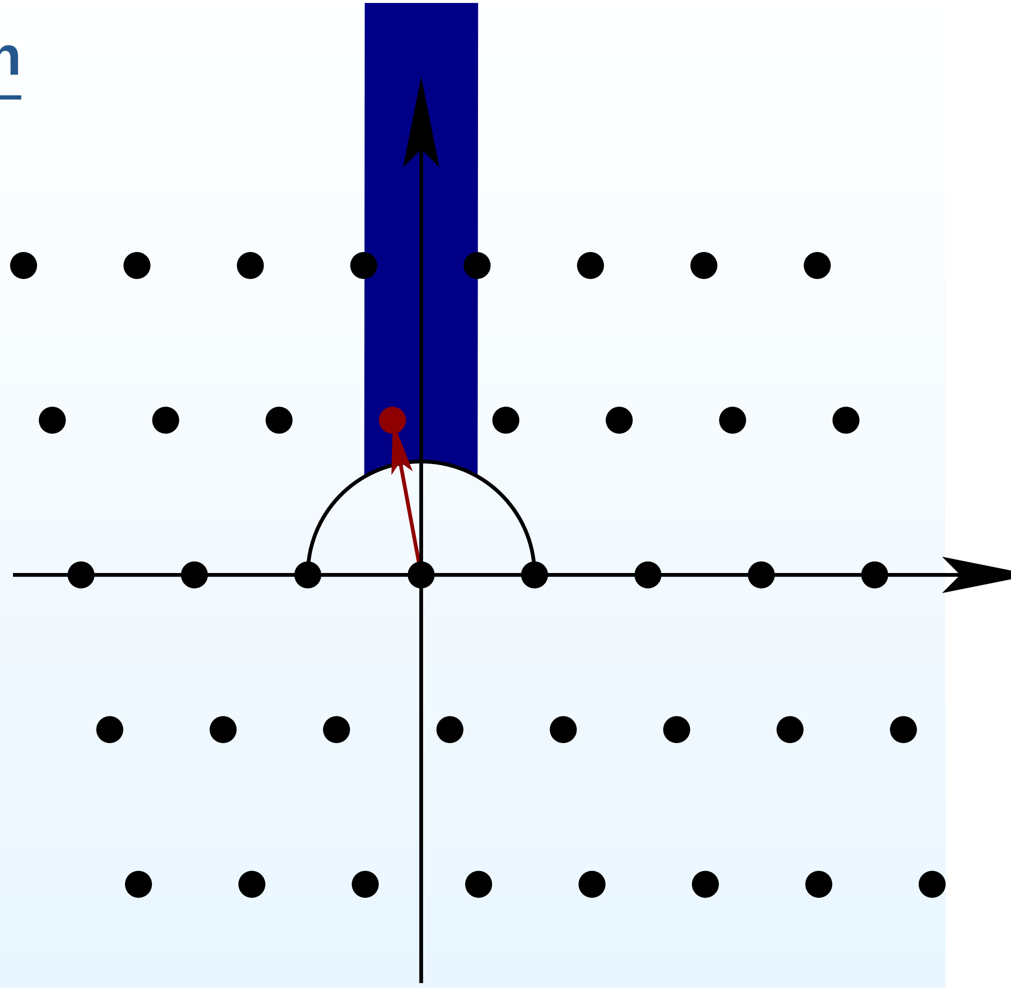

Space of lattices: fundamental domain

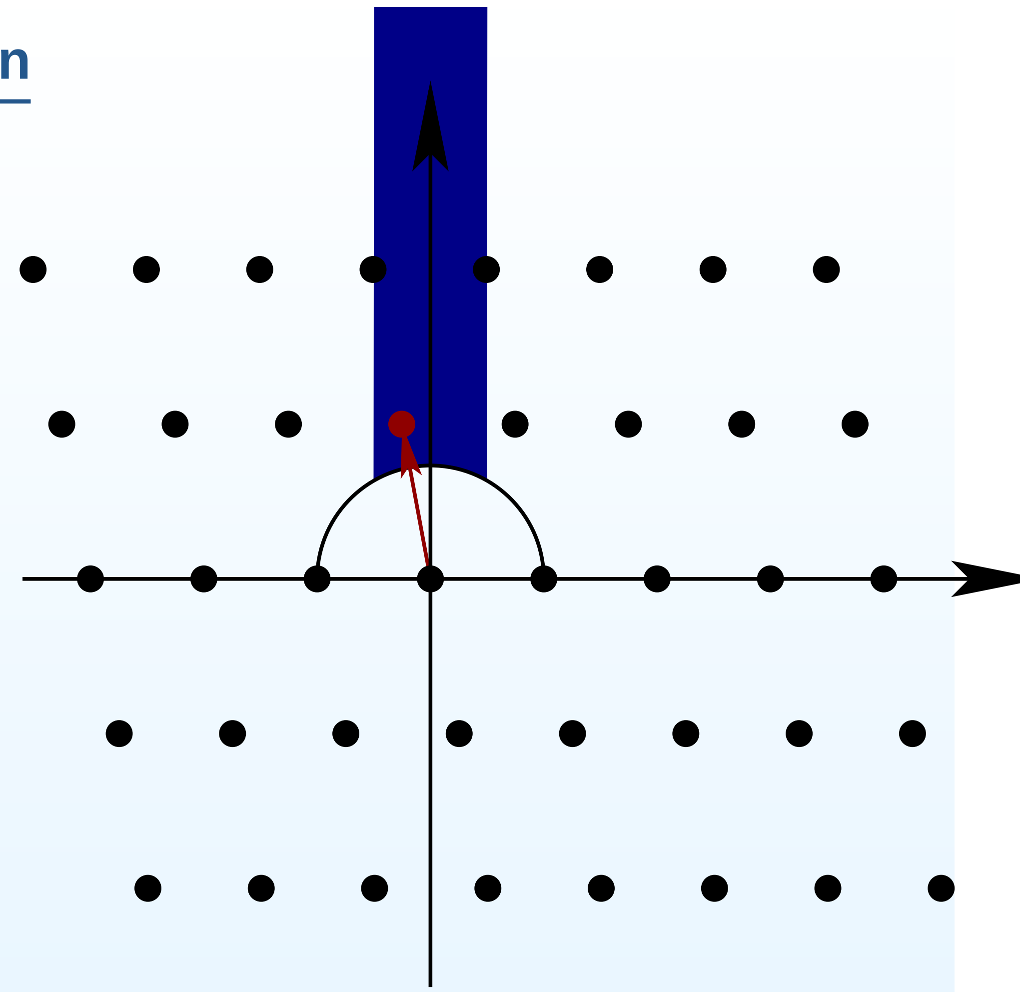

- Choosing an appropriate homothety and rotation we can place the shortest vector of the lattice to the horizontal unit vector.
- Consider the shortest vector of the lattice located in the upper half-plane.
- It lives outside the unit disc.
- It belongs to the strip $-1/2 \leq x \leq 1/2$.

We have constructed a fundamental domain in the space of lattices.

Family of flat tori

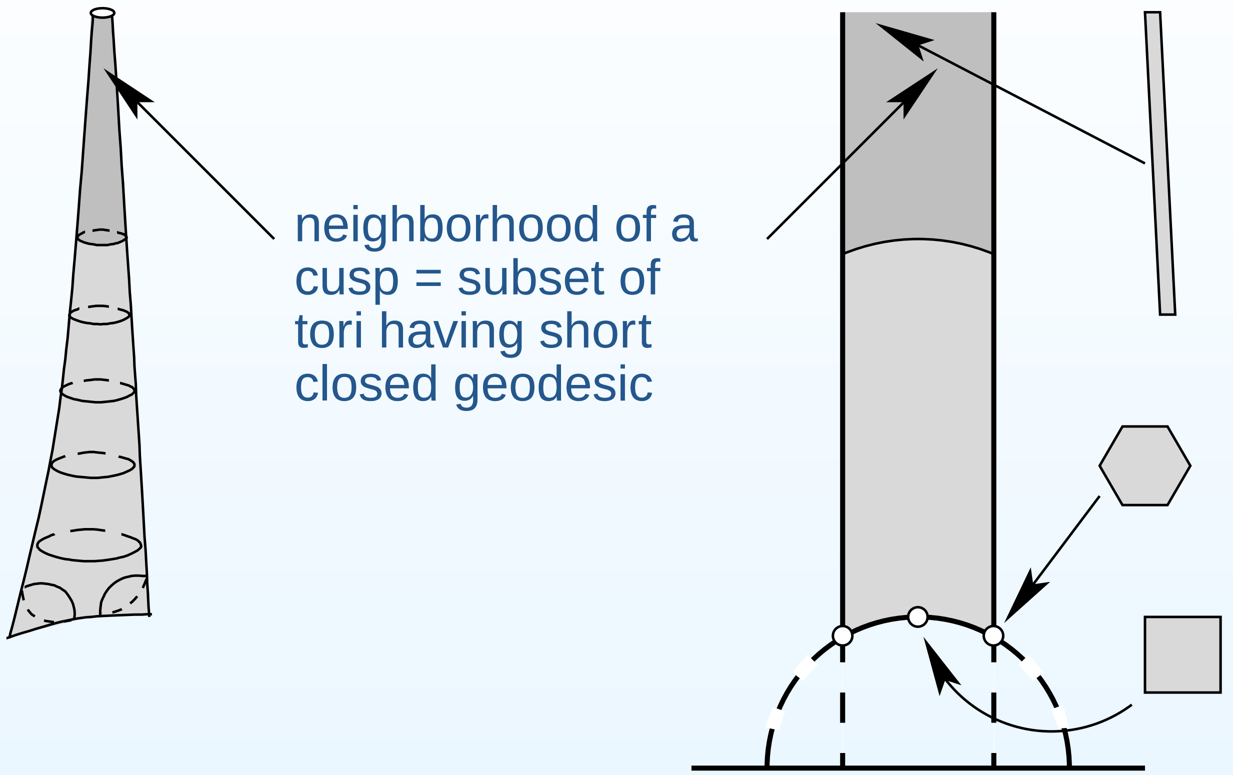

The corresponding “modular surface” is not compact: flat tori representing points, which are close to the cusp, are almost degenerate: they have a very short closed geodesic.

The modular surface inherits the hyperbolic metric from the upper half-plane.

Family of flat tori

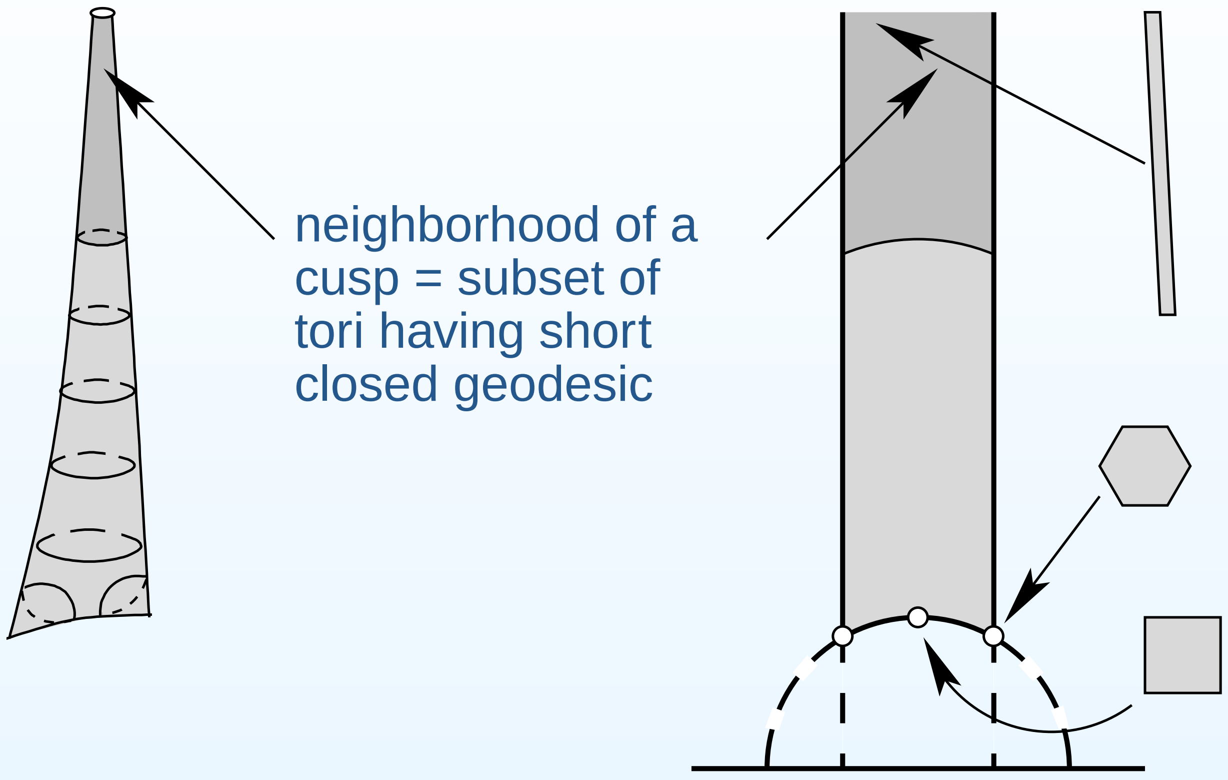

The corresponding “modular surface” is not compact: flat tori representing points, which are close to the cusp, are almost degenerate: they have a very short closed geodesic.

The modular surface inherits the hyperbolic metric from the upper half-plane.

Diffeomorphisms of surfaces

Diffeomorphisms of surfaces

Observation 1. *Surfaces can wrap around themselves.*

Cut a torus along a horizontal circle.

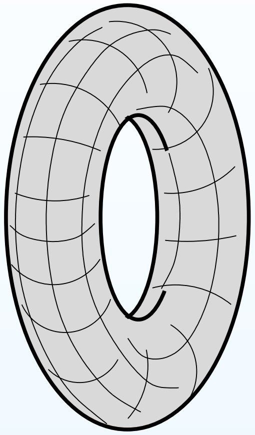

Diffeomorphisms of surfaces

Observation 1. *Surfaces can wrap around themselves.*

Dehn twist twists progressively horizontal circles up to a complete turn on the opposite boundary component of the cylinder and then identifies the components.

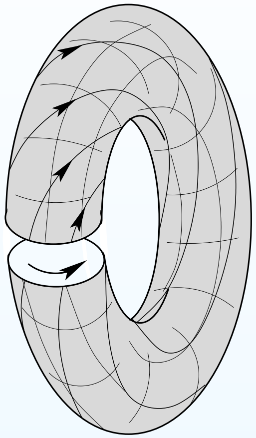

Diffeomorphisms of surfaces

Observation 1. *Surfaces can wrap around themselves.*

Dehn twist twists progressively horizontal circles up to a complete turn on the opposite boundary component of the cylinder and then identifies the components.

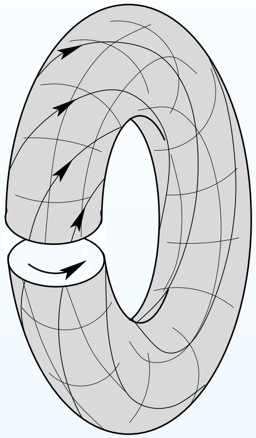

$$\begin{array}{ccc} \mathbb{R}^2 & \xrightarrow{\hat{f}_h} & \mathbb{R}^2 \\ \downarrow & & \downarrow \\ \mathbb{R}^2/\mathbb{Z}^2 = \mathbb{T}^2 & \xrightarrow[f_h]{} & \mathbb{T}^2 = \mathbb{R}^2/\mathbb{Z}^2 \end{array}$$

Dehn twist corresponds to the linear map $\hat{f}_h : \mathbb{R}^2 \to \mathbb{R}^2$ with the matrix $\begin{pmatrix} 1 & 1 \\ 0 & 1 \end{pmatrix}$.

Diffeomorphisms of surfaces

Observation 1. *Surfaces can wrap around themselves.*

Dehn twist twists progressively horizontal circles up to a complete turn on the opposite boundary component of the cylinder and then identifies the components.

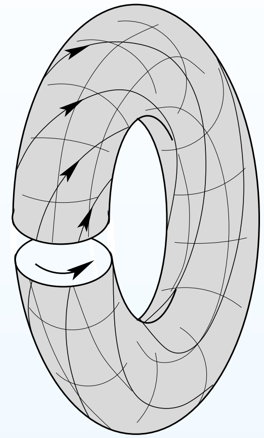

$$\begin{array}{ccc} \mathbb{R}^2 & \xrightarrow{\hat{f}_h} & \mathbb{R}^2 \\ \downarrow & & \downarrow \\ \mathbb{R}^2/\mathbb{Z}^2 = \mathbb{T}^2 & \xrightarrow[f_h]{} & \mathbb{T}^2 = \mathbb{R}^2/\mathbb{Z}^2 \end{array}$$

Dehn twist corresponds to the linear map $\hat{f}_h : \mathbb{R}^2 \to \mathbb{R}^2$ with the matrix $\begin{pmatrix} 1 & 1 \\ 0 & 1 \end{pmatrix}$.

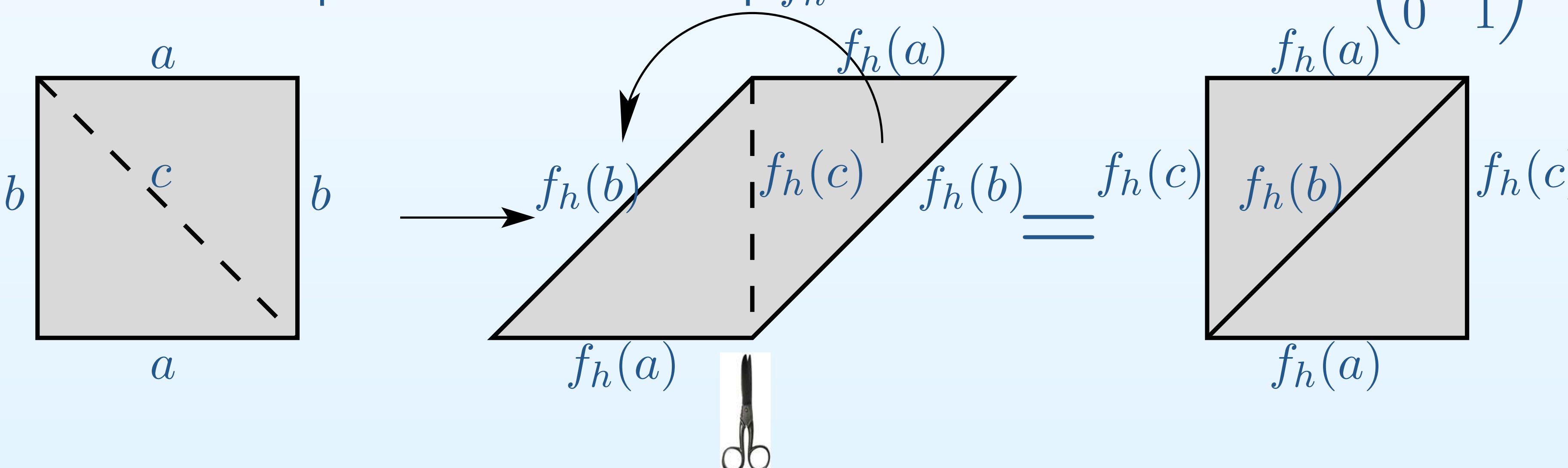

It maps the square pattern of the torus to a parallelogram pattern. Cutting and pasting appropriately we can transform the new pattern to the initial square.

Diffeomorphisms of surfaces

Observation 1. *Surfaces can wrap around themselves.*

Dehn twist twists progressively horizontal circles up to a complete turn on the opposite boundary component of the cylinder and then identifies the components.

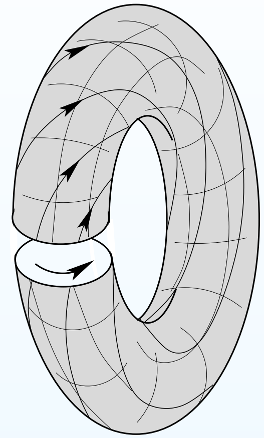

$$\begin{array}{ccc} \mathbb{R}^2 & \xrightarrow{\hat{f}_h} & \mathbb{R}^2 \\ \downarrow & & \downarrow \\ \mathbb{R}^2/\mathbb{Z}^2 = \mathbb{T}^2 & \xrightarrow[f_h]{} & \mathbb{T}^2 = \mathbb{R}^2/\mathbb{Z}^2 \end{array}$$

Dehn twist corresponds to the linear map $\hat{f}_h : \mathbb{R}^2 \to \mathbb{R}^2$ with the matrix $\begin{pmatrix} 1 & 1 \\ 0 & 1 \end{pmatrix}$.

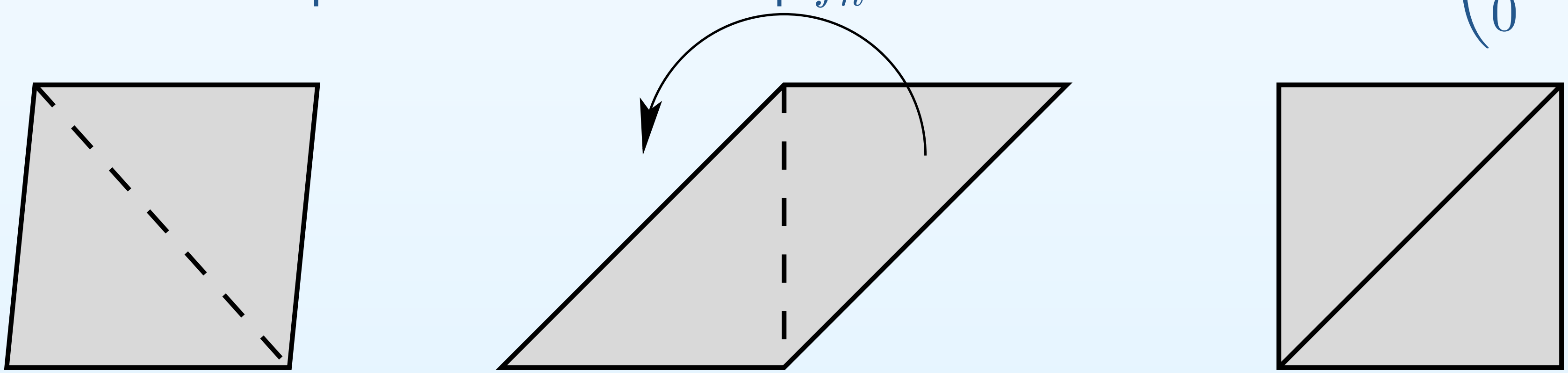

Changing the slope of the parallelogram pattern progressively we get a *closed path* in the space of flat tori.

Diffeomorphisms of surfaces

Observation 1. *Surfaces can wrap around themselves.*

Dehn twist twists progressively horizontal circles up to a complete turn on the opposite boundary component of the cylinder and then identifies the components.

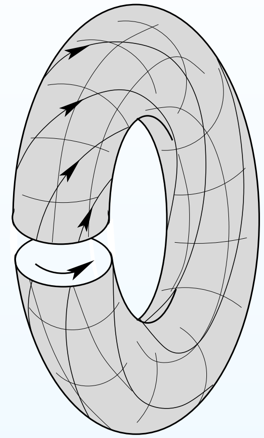

$$\begin{array}{ccc} \mathbb{R}^2 & \xrightarrow{\hat{f}_h} & \mathbb{R}^2 \\ \downarrow & & \downarrow \\ \mathbb{R}^2/\mathbb{Z}^2 = \mathbb{T}^2 & \xrightarrow[f_h]{} & \mathbb{T}^2 = \mathbb{R}^2/\mathbb{Z}^2 \end{array}$$

Dehn twist corresponds to the linear map $\hat{f}_h : \mathbb{R}^2 \to \mathbb{R}^2$ with the matrix $\begin{pmatrix} 1 & 1 \\ 0 & 1 \end{pmatrix}$.

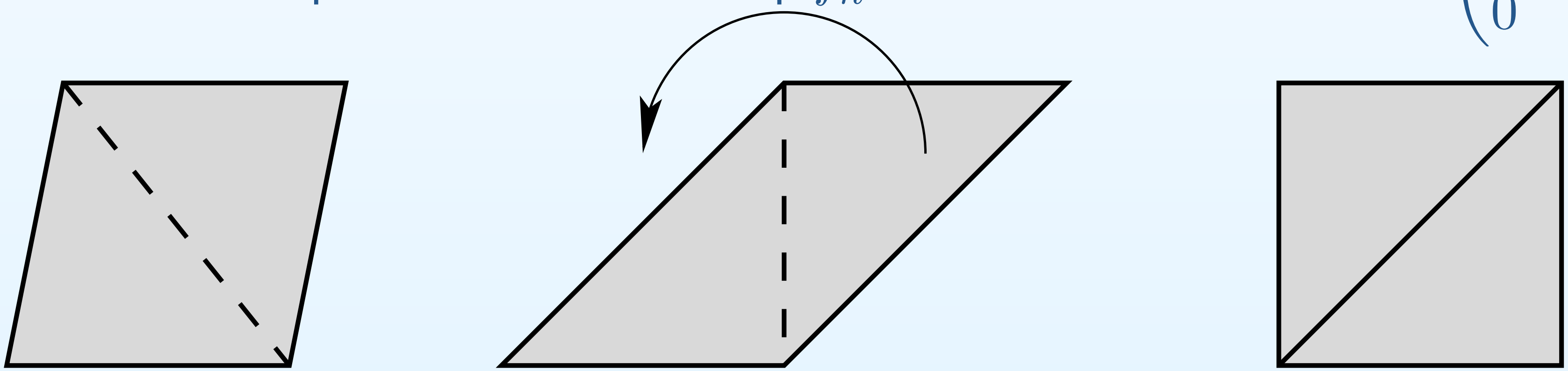

Changing the slope of the parallelogram pattern progressively we get a *closed path* in the space of flat tori.

Diffeomorphisms of surfaces

Observation 1. *Surfaces can wrap around themselves.*

Dehn twist twists progressively horizontal circles up to a complete turn on the opposite boundary component of the cylinder and then identifies the components.

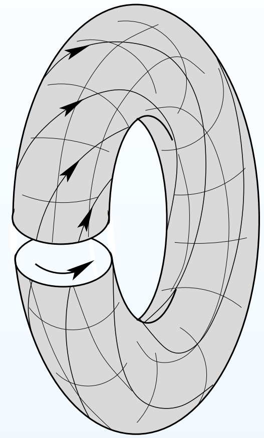

$$\begin{array}{ccc} \mathbb{R}^2 & \xrightarrow{\hat{f}_h} & \mathbb{R}^2 \\ \downarrow & & \downarrow \\ \mathbb{R}^2/\mathbb{Z}^2 = \mathbb{T}^2 & \xrightarrow[f_h]{} & \mathbb{T}^2 = \mathbb{R}^2/\mathbb{Z}^2 \end{array}$$

Dehn twist corresponds to the linear map $\hat{f}_h : \mathbb{R}^2 \to \mathbb{R}^2$ with the matrix $\begin{pmatrix} 1 & 1 \\ 0 & 1 \end{pmatrix}$.

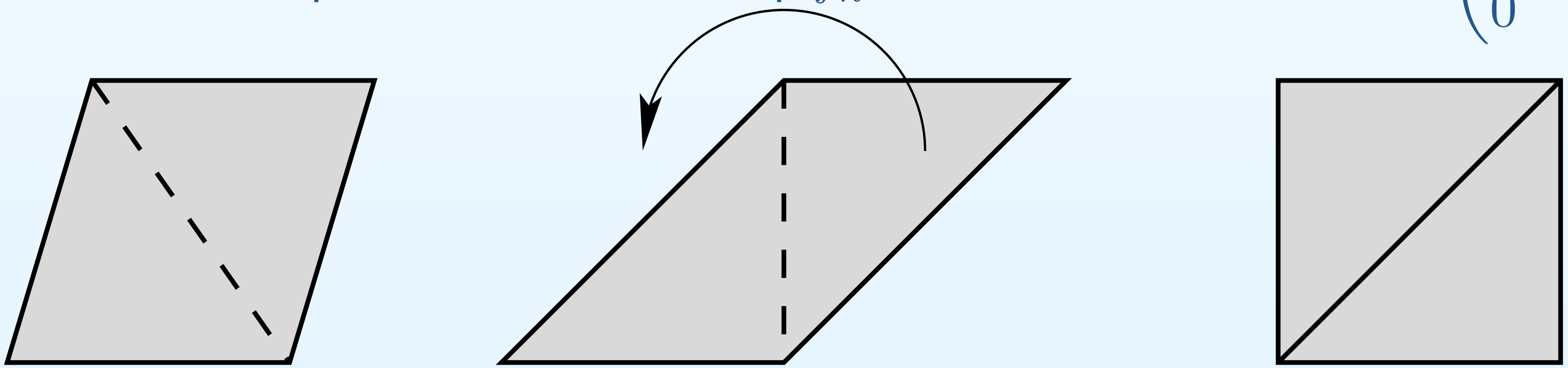

Changing the slope of the parallelogram pattern progressively we get a *closed path* in the space of flat tori.

Diffeomorphisms of surfaces

Observation 1. *Surfaces can wrap around themselves.*

Dehn twist twists progressively horizontal circles up to a complete turn on the opposite boundary component of the cylinder and then identifies the components.

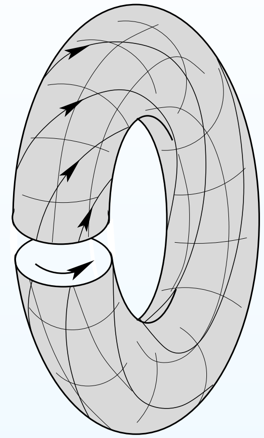

$$\begin{array}{ccc} \mathbb{R}^2 & \xrightarrow{\hat{f}_h} & \mathbb{R}^2 \\ \downarrow & & \downarrow \\ \mathbb{R}^2/\mathbb{Z}^2 = \mathbb{T}^2 & \xrightarrow[f_h]{} & \mathbb{T}^2 = \mathbb{R}^2/\mathbb{Z}^2 \end{array}$$

Dehn twist corresponds to the linear map $\hat{f}_h : \mathbb{R}^2 \to \mathbb{R}^2$ with the matrix $\begin{pmatrix} 1 & 1 \\ 0 & 1 \end{pmatrix}$.

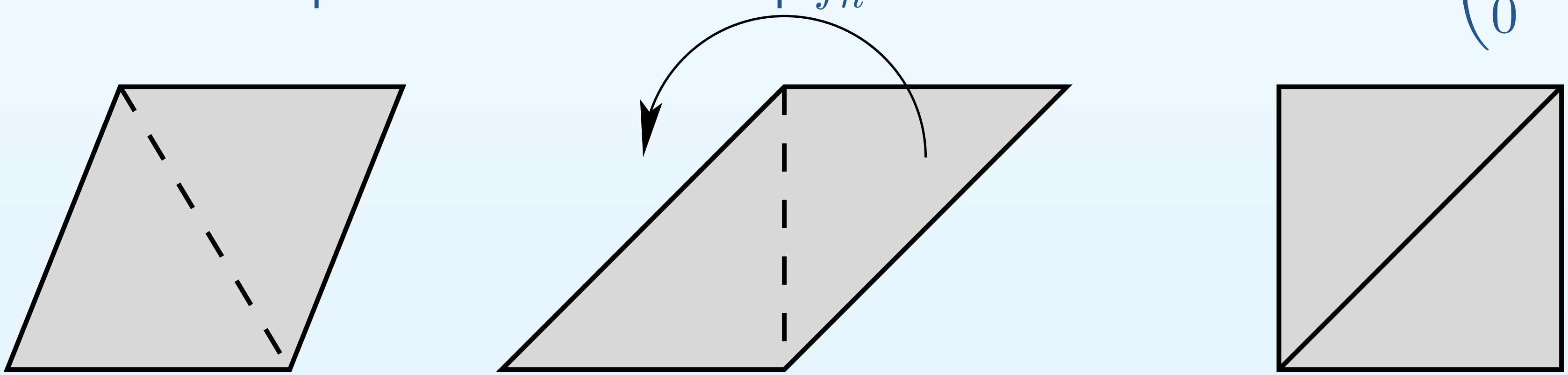

Changing the slope of the parallelogram pattern progressively we get a *closed path* in the space of flat tori.

Diffeomorphisms of surfaces

Observation 1. *Surfaces can wrap around themselves.*

Dehn twist twists progressively horizontal circles up to a complete turn on the opposite boundary component of the cylinder and then identifies the components.

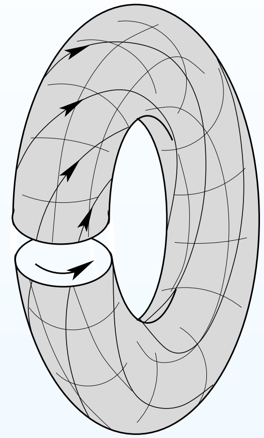

$$\begin{array}{ccc} \mathbb{R}^2 & \xrightarrow{\hat{f}_h} & \mathbb{R}^2 \\ \downarrow & & \downarrow \\ \mathbb{R}^2/\mathbb{Z}^2 = \mathbb{T}^2 & \xrightarrow[f_h]{} & \mathbb{T}^2 = \mathbb{R}^2/\mathbb{Z}^2 \end{array}$$

Dehn twist corresponds to the linear map $\hat{f}_h : \mathbb{R}^2 \to \mathbb{R}^2$ with the matrix $\begin{pmatrix} 1 & 1 \\ 0 & 1 \end{pmatrix}$.

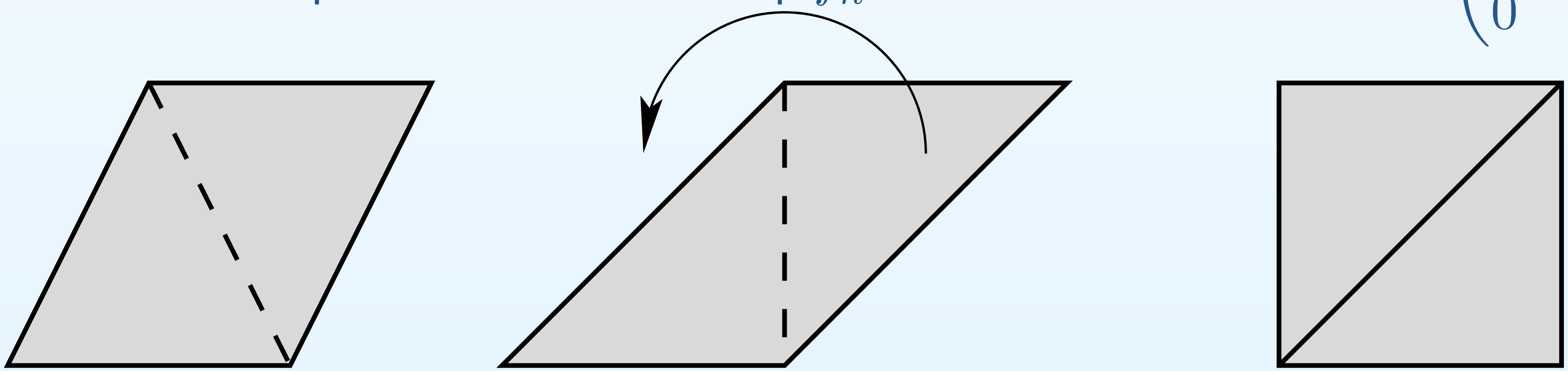

Changing the slope of the parallelogram pattern progressively we get a *closed path* in the space of flat tori.

Diffeomorphisms of surfaces

Observation 1. *Surfaces can wrap around themselves.*

Dehn twist twists progressively horizontal circles up to a complete turn on the opposite boundary component of the cylinder and then identifies the components.

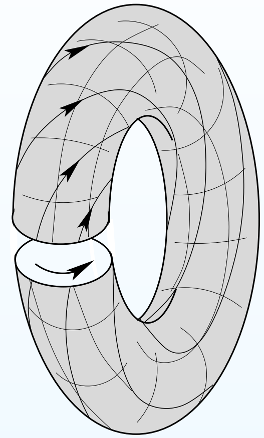

$$\begin{array}{ccc} \mathbb{R}^2 & \xrightarrow{\hat{f}_h} & \mathbb{R}^2 \\ \downarrow & & \downarrow \\ \mathbb{R}^2/\mathbb{Z}^2 = \mathbb{T}^2 & \xrightarrow[f_h]{} & \mathbb{T}^2 = \mathbb{R}^2/\mathbb{Z}^2 \end{array}$$

Dehn twist corresponds to the linear map $\hat{f}_h : \mathbb{R}^2 \to \mathbb{R}^2$ with the matrix $\begin{pmatrix} 1 & 1 \\ 0 & 1 \end{pmatrix}$.

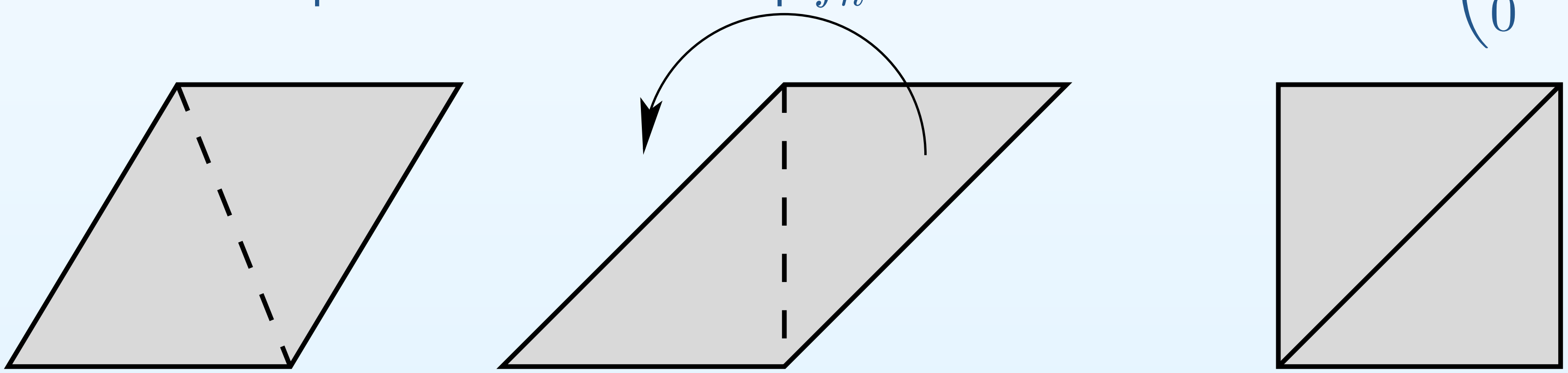

Changing the slope of the parallelogram pattern progressively we get a *closed path* in the space of flat tori.

Diffeomorphisms of surfaces

Observation 1. *Surfaces can wrap around themselves.*

Dehn twist twists progressively horizontal circles up to a complete turn on the opposite boundary component of the cylinder and then identifies the components.

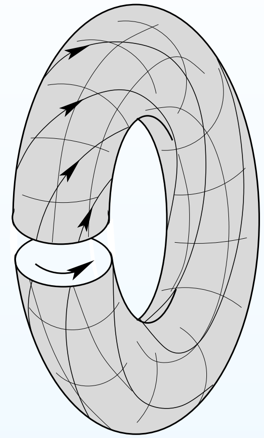

$$\begin{array}{ccc} \mathbb{R}^2 & \xrightarrow{\hat{f}_h} & \mathbb{R}^2 \\ \downarrow & & \downarrow \\ \mathbb{R}^2/\mathbb{Z}^2 = \mathbb{T}^2 & \xrightarrow[f_h]{} & \mathbb{T}^2 = \mathbb{R}^2/\mathbb{Z}^2 \end{array}$$

Dehn twist corresponds to the linear map $\hat{f}_h : \mathbb{R}^2 \to \mathbb{R}^2$ with the matrix $\begin{pmatrix} 1 & 1 \\ 0 & 1 \end{pmatrix}$.

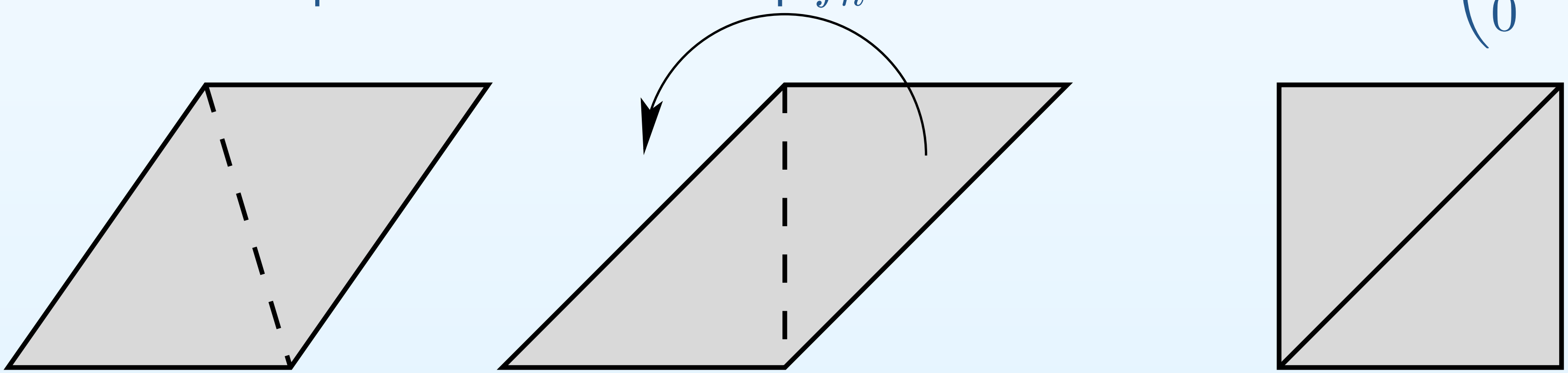

Changing the slope of the parallelogram pattern progressively we get a *closed path* in the space of flat tori.

Diffeomorphisms of surfaces

Observation 1. *Surfaces can wrap around themselves.*

Dehn twist twists progressively horizontal circles up to a complete turn on the opposite boundary component of the cylinder and then identifies the components.

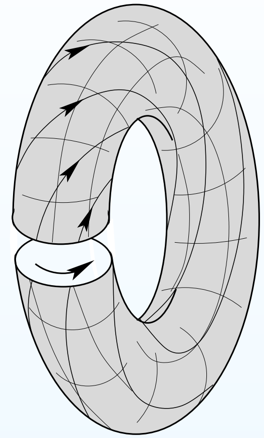

$$\begin{array}{ccc} \mathbb{R}^2 & \xrightarrow{\hat{f}_h} & \mathbb{R}^2 \\ \downarrow & & \downarrow \\ \mathbb{R}^2/\mathbb{Z}^2 = \mathbb{T}^2 & \xrightarrow[f_h]{} & \mathbb{T}^2 = \mathbb{R}^2/\mathbb{Z}^2 \end{array}$$

Dehn twist corresponds to the linear map $\hat{f}_h : \mathbb{R}^2 \to \mathbb{R}^2$ with the matrix $\begin{pmatrix} 1 & 1 \\ 0 & 1 \end{pmatrix}$.

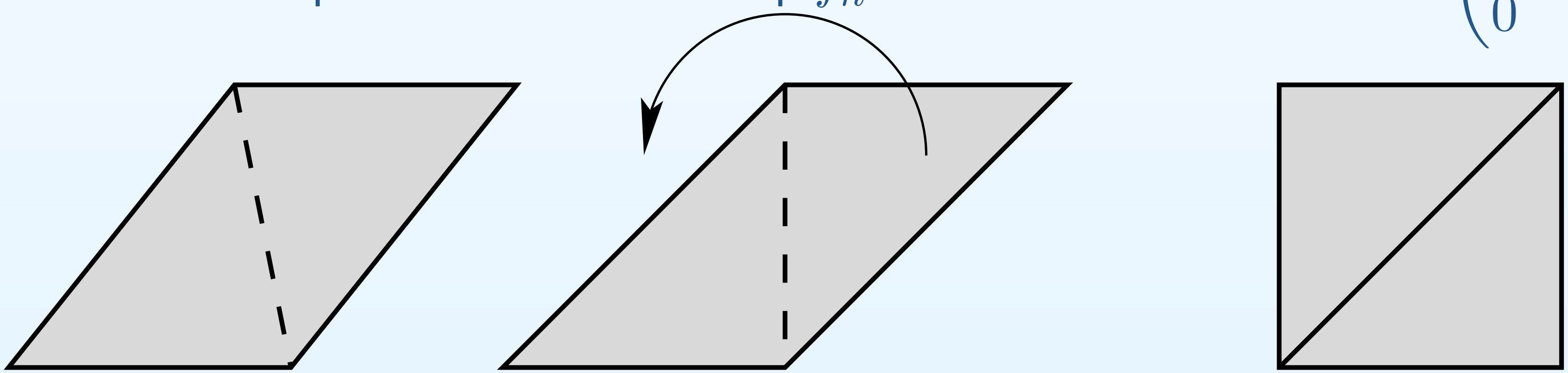

Changing the slope of the parallelogram pattern progressively we get a *closed path* in the space of flat tori.

Diffeomorphisms of surfaces

Observation 1. *Surfaces can wrap around themselves.*

Dehn twist twists progressively horizontal circles up to a complete turn on the opposite boundary component of the cylinder and then identifies the components.

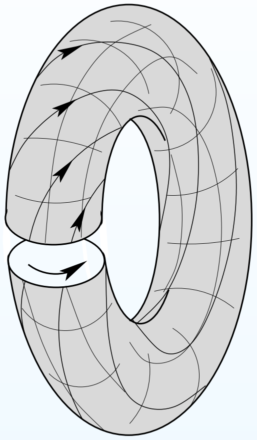

$$\begin{array}{ccc} \mathbb{R}^2 & \xrightarrow{\hat{f}_h} & \mathbb{R}^2 \\ \downarrow & & \downarrow \\ \mathbb{R}^2/\mathbb{Z}^2 = \mathbb{T}^2 & \xrightarrow[f_h]{} & \mathbb{T}^2 = \mathbb{R}^2/\mathbb{Z}^2 \end{array}$$

Dehn twist corresponds to the linear map $\hat{f}_h : \mathbb{R}^2 \to \mathbb{R}^2$ with the matrix $\begin{pmatrix} 1 & 1 \\ 0 & 1 \end{pmatrix}$.

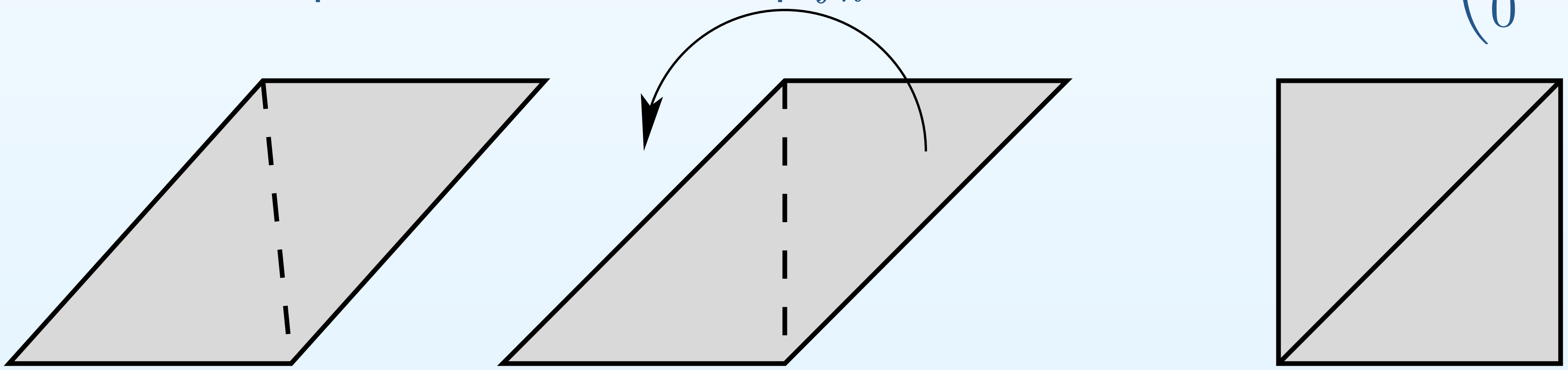

Changing the slope of the parallelogram pattern progressively we get a *closed path* in the space of flat tori.

Diffeomorphisms of surfaces

Observation 1. *Surfaces can wrap around themselves.*

Dehn twist twists progressively horizontal circles up to a complete turn on the opposite boundary component of the cylinder and then identifies the components.

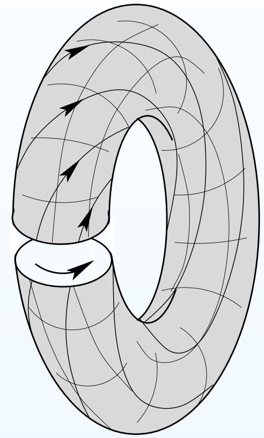

$$\begin{array}{ccc} \mathbb{R}^2 & \xrightarrow{\hat{f}_h} & \mathbb{R}^2 \\ \downarrow & & \downarrow \\ \mathbb{R}^2/\mathbb{Z}^2 = \mathbb{T}^2 & \xrightarrow[f_h]{} & \mathbb{T}^2 = \mathbb{R}^2/\mathbb{Z}^2 \end{array}$$

Dehn twist corresponds to the linear map $\hat{f}_h : \mathbb{R}^2 \to \mathbb{R}^2$ with the matrix $\begin{pmatrix} 1 & 1 \\ 0 & 1 \end{pmatrix}$.

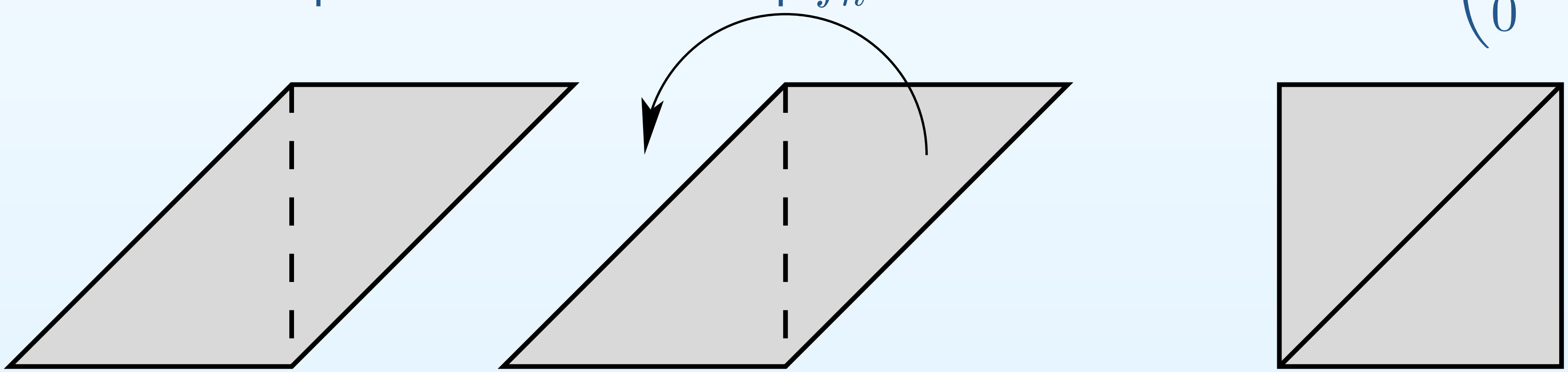

Changing the slope of the parallelogram pattern progressively we get a *closed path* in the space of flat tori.

Diffeomorphisms of surfaces

Observation 1. *Surfaces can wrap around themselves.*

Dehn twist twists progressively horizontal circles up to a complete turn on the opposite boundary component of the cylinder and then identifies the components.

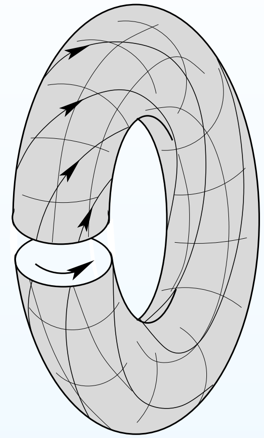

$$\begin{array}{ccc} \mathbb{R}^2 & \xrightarrow{\hat{f}_h} & \mathbb{R}^2 \\ \downarrow & & \downarrow \\ \mathbb{R}^2/\mathbb{Z}^2 = \mathbb{T}^2 & \xrightarrow[f_h]{} & \mathbb{T}^2 = \mathbb{R}^2/\mathbb{Z}^2 \end{array}$$

Dehn twist corresponds to the linear map $\hat{f}_h : \mathbb{R}^2 \to \mathbb{R}^2$ with the matrix $\begin{pmatrix} 1 & 1 \\ 0 & 1 \end{pmatrix}$.

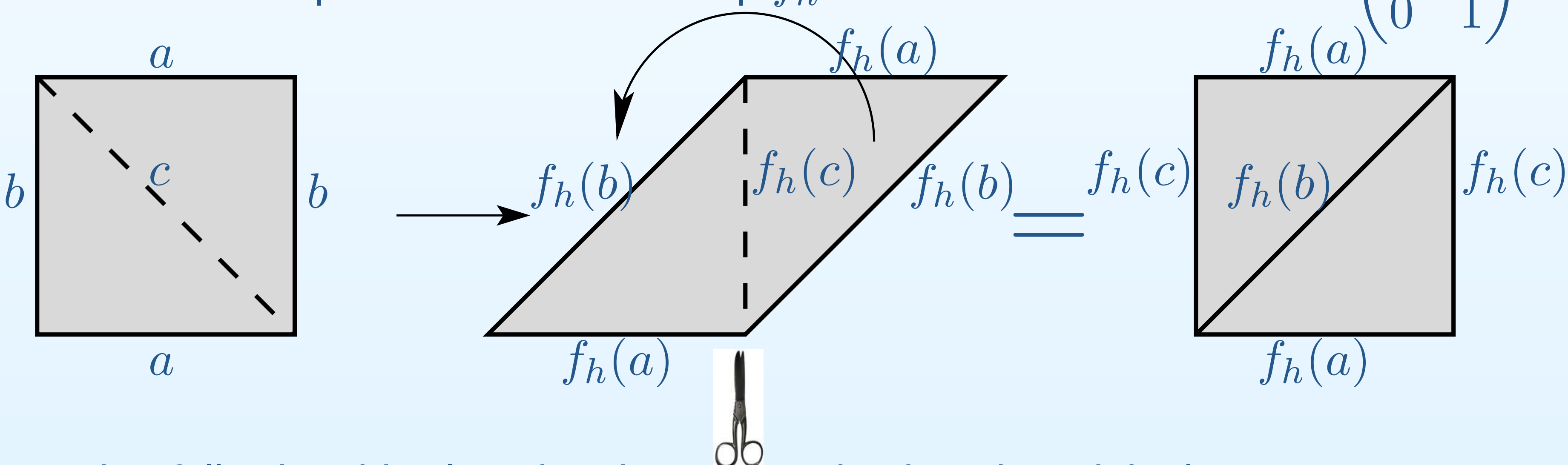

Note that following this closed path we come back to the original square torus having twisted the homology!

Closed horocycle in the moduli space of tori

Projection of a similar closed orbit of the *horocyclic flow* $\begin{pmatrix} 1 & t \\ 0 & 1 \end{pmatrix}$ to the moduli space of flat tori.

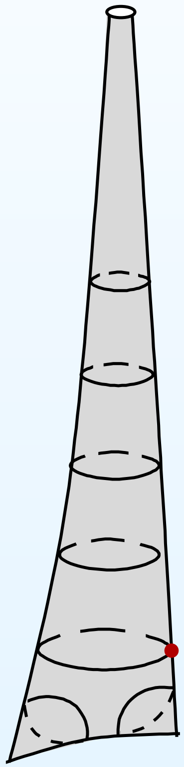

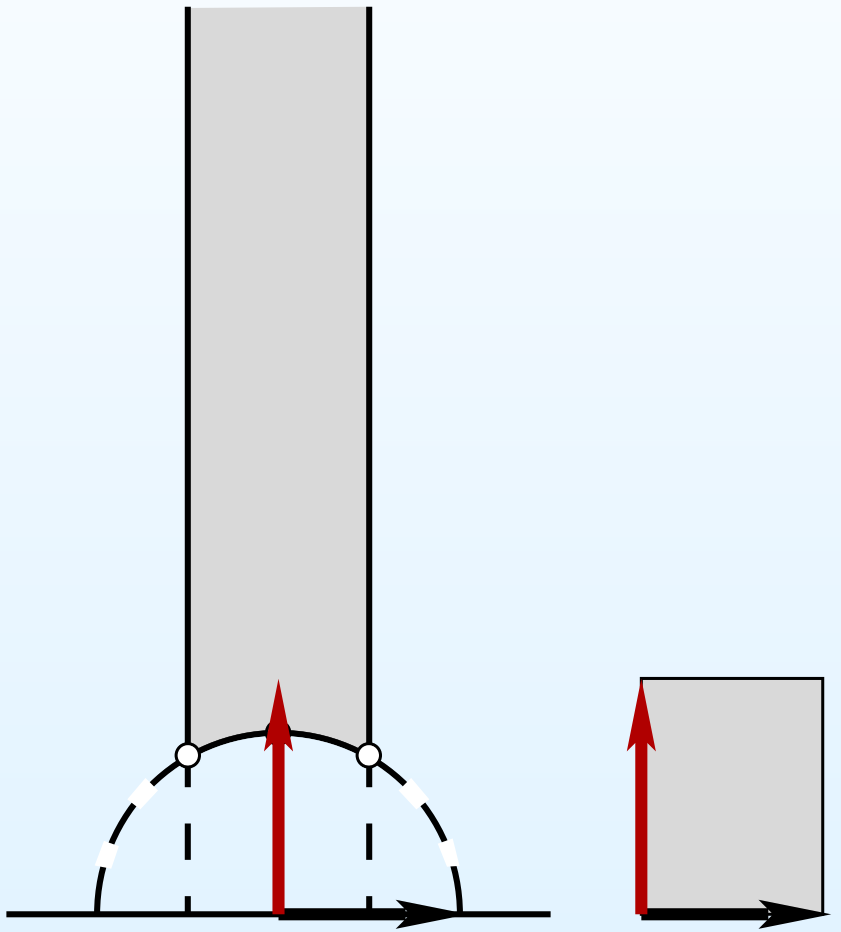

Closed horocycle in the moduli space of tori

Projection of a similar closed orbit of the *horocyclic flow* $\begin{pmatrix} 1 & t \\ 0 & 1 \end{pmatrix}$ to the moduli space of flat tori.

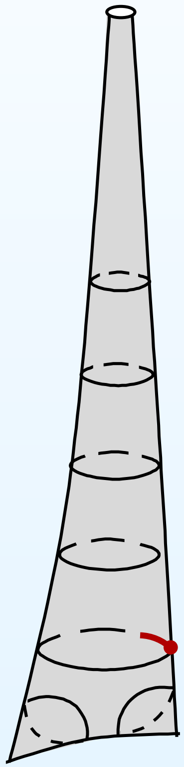

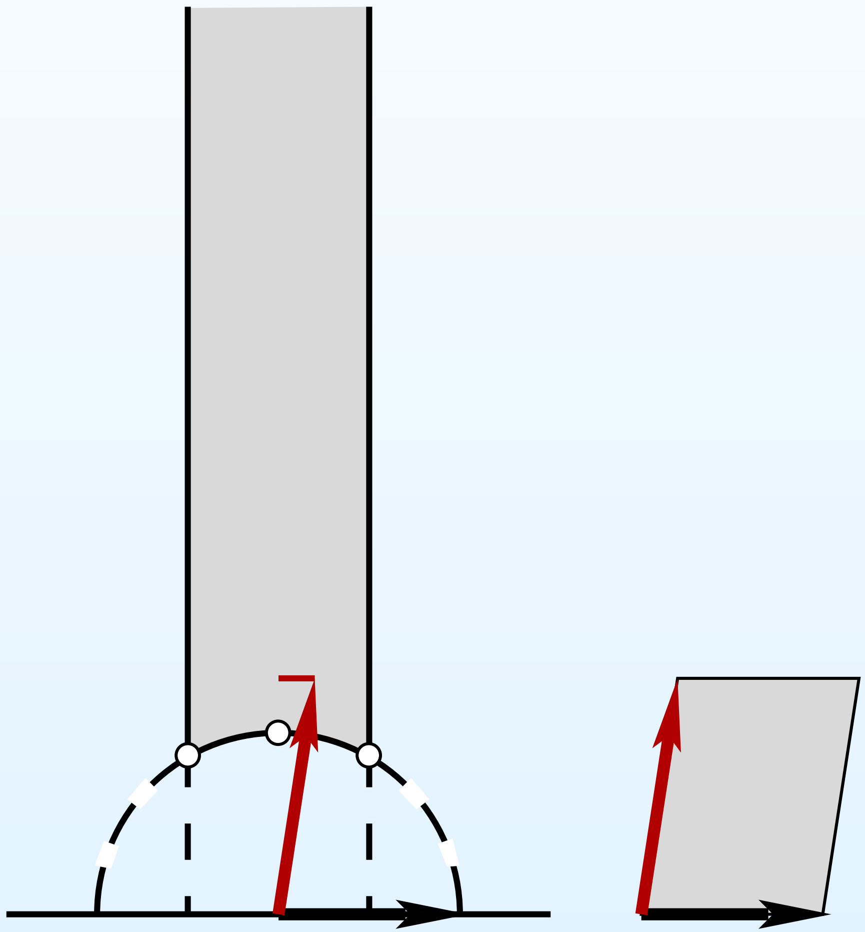

Closed horocycle in the moduli space of tori

Projection of a similar closed orbit of the *horocyclic flow* $\begin{pmatrix} 1 & t \\ 0 & 1 \end{pmatrix}$ to the moduli space of flat tori.

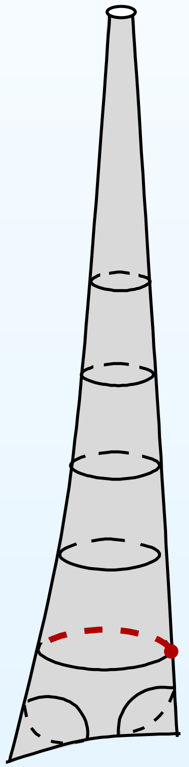

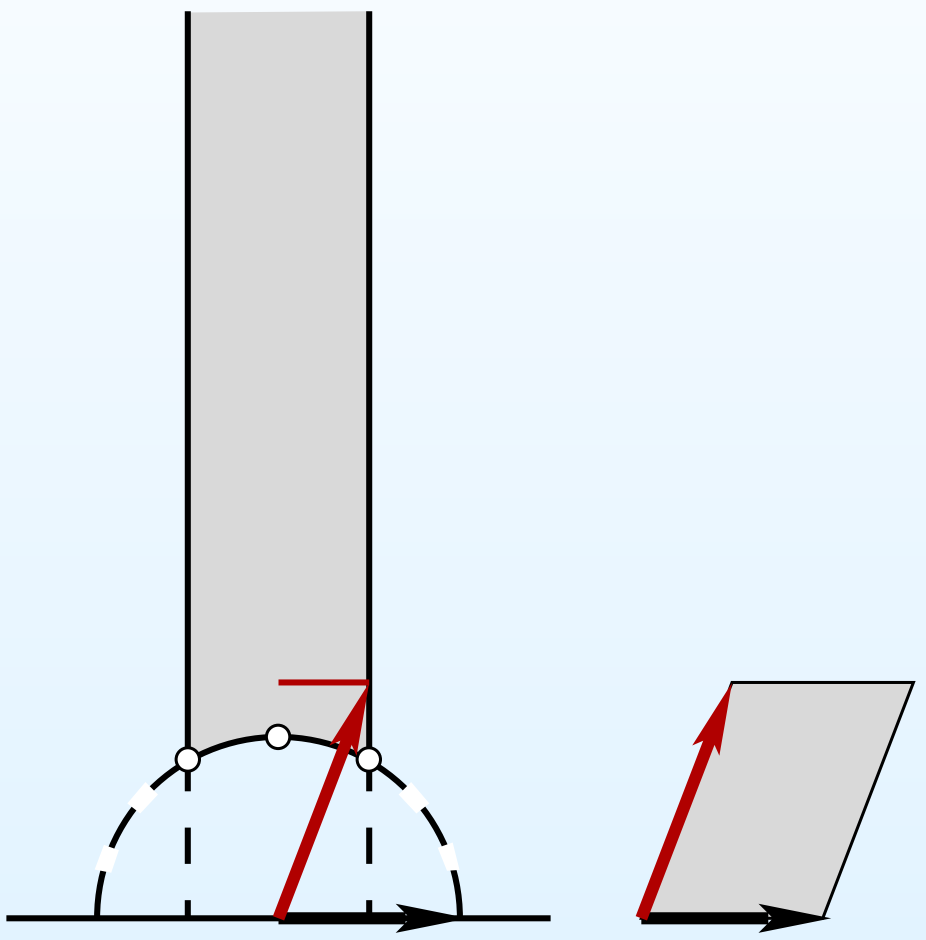

Closed horocycle in the moduli space of tori

Projection of a similar closed orbit of the *horocyclic flow* $\begin{pmatrix} 1 & t \\ 0 & 1 \end{pmatrix}$ to the moduli space of flat tori.

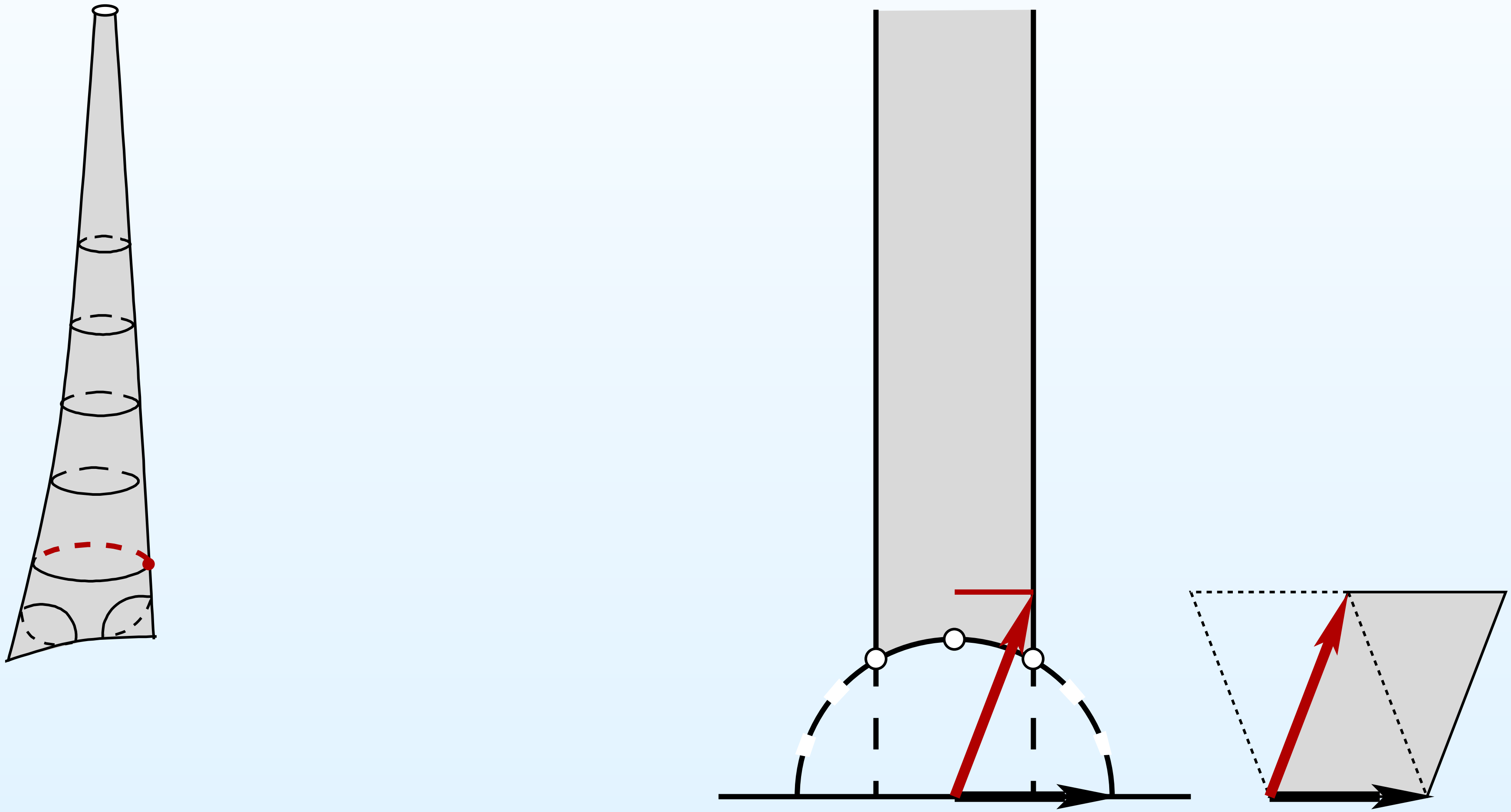

Closed horocycle in the moduli space of tori

Projection of a similar closed orbit of the *horocyclic flow* $\begin{pmatrix} 1 & t \\ 0 & 1 \end{pmatrix}$ to the moduli space of flat tori.

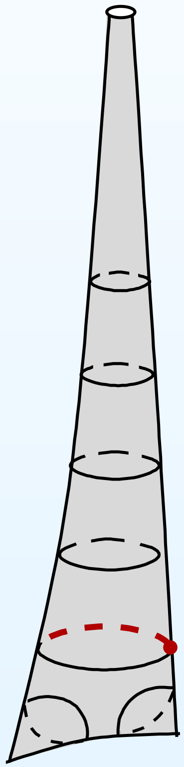

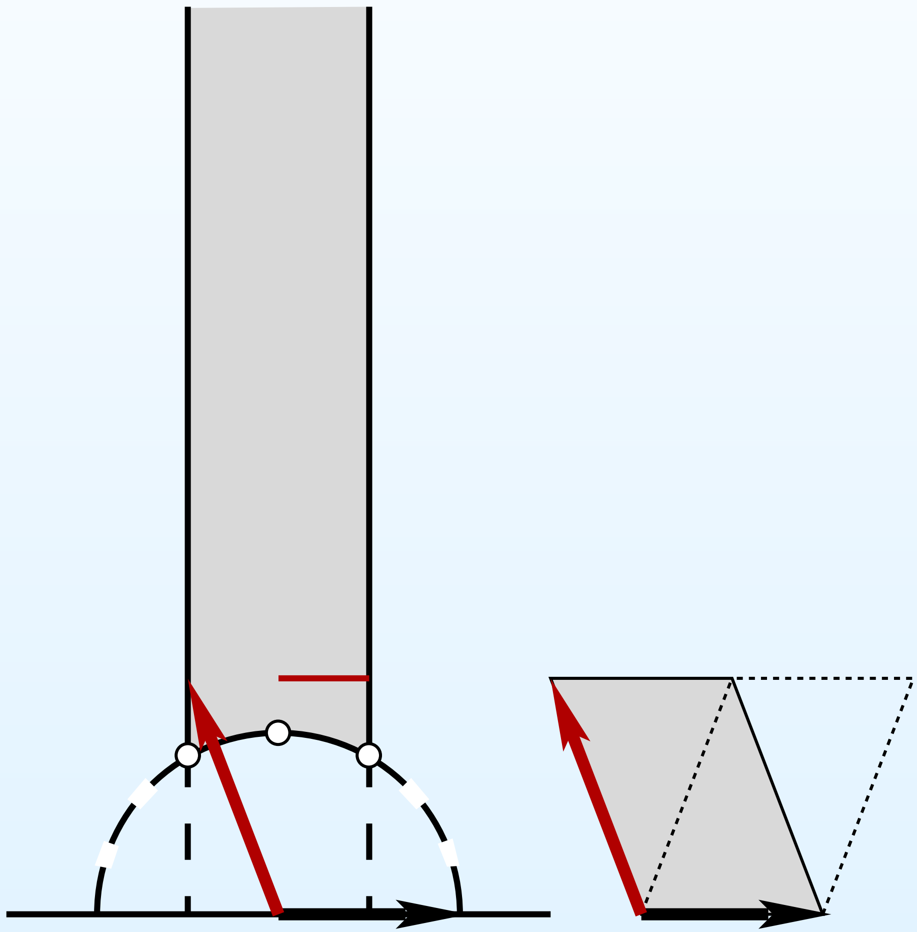

Closed horocycle in the moduli space of tori

Projection of a similar closed orbit of the *horocyclic flow* $\begin{pmatrix} 1 & t \\ 0 & 1 \end{pmatrix}$ to the moduli space of flat tori.

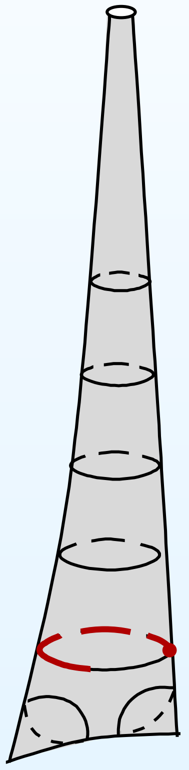

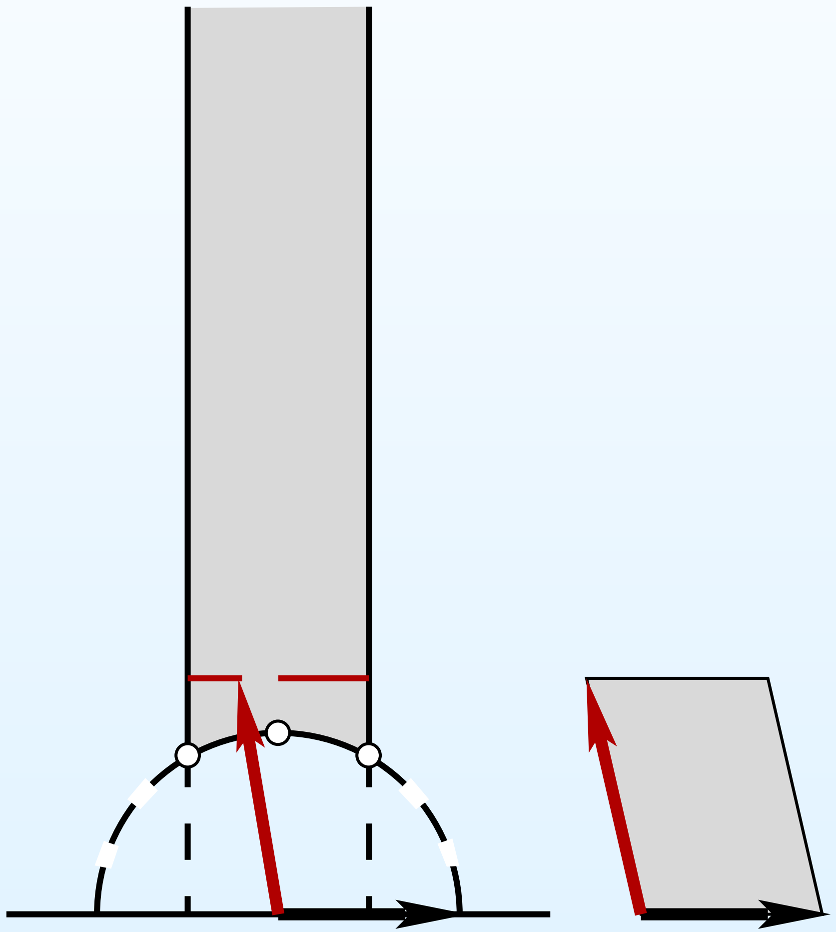

Closed horocycle in the moduli space of tori

Projection of a similar closed orbit of the *horocyclic flow* $\begin{pmatrix} 1 & t \\ 0 & 1 \end{pmatrix}$ to the moduli space of flat tori.

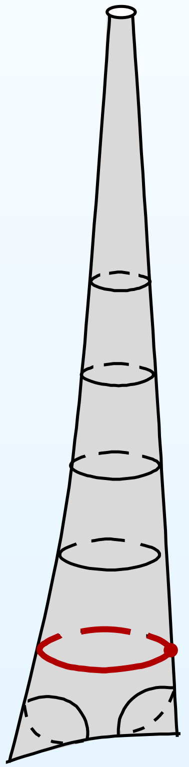

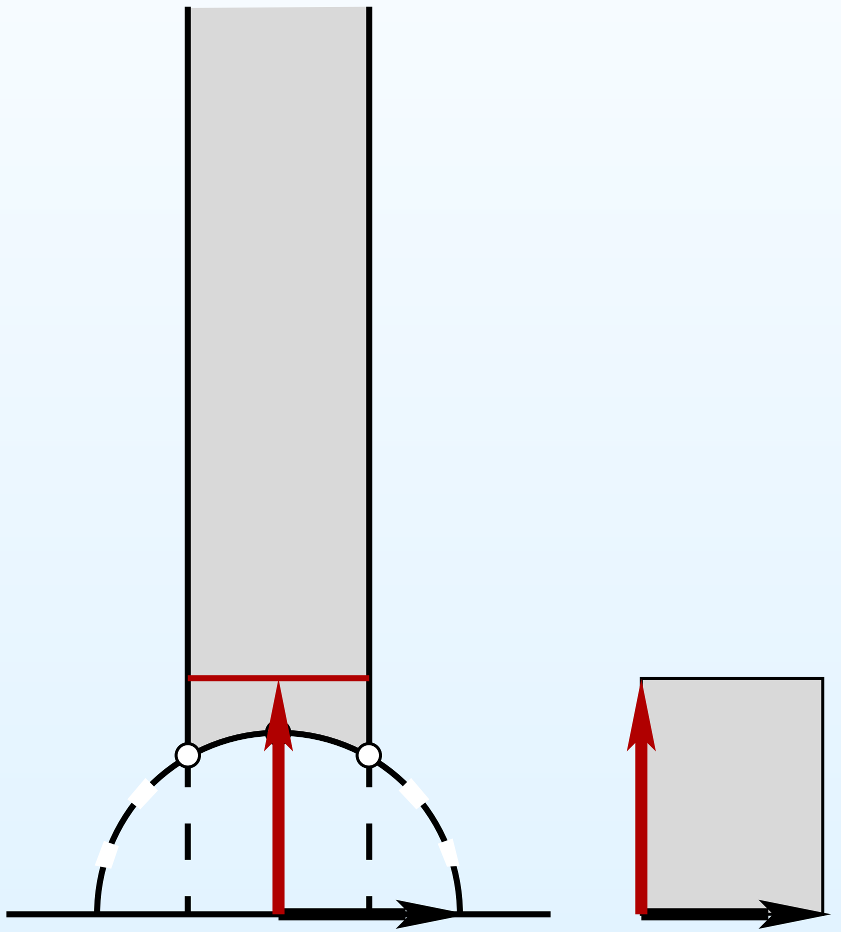

Pseudo-Anosov diffeomorphisms

Consider a composition
of two Dehn twists

$$g = f_v \circ f_h =$$ 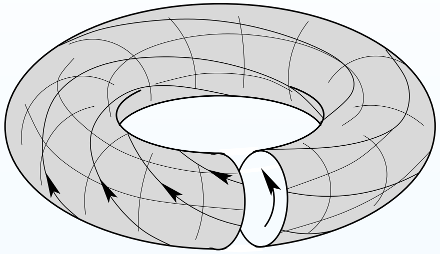 $\circ$ 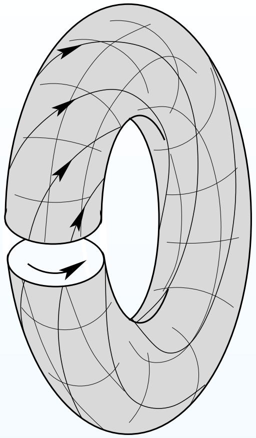

Consider a composition of two Dehn twists $g = f_v \circ f_h =$

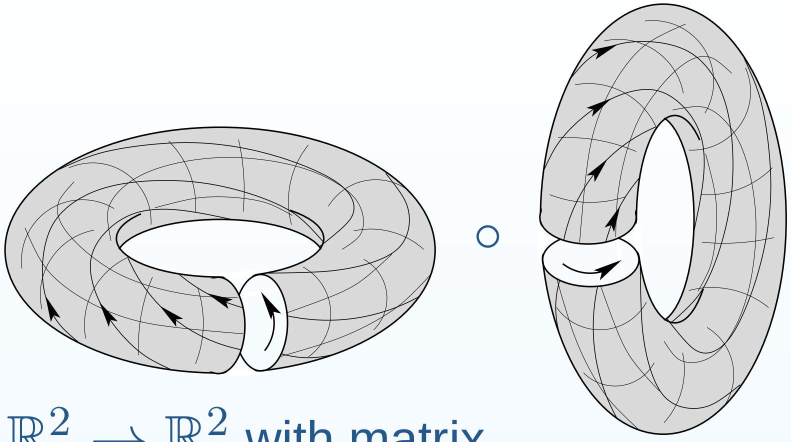

It corresponds to the integer linear map $\hat{g} : \mathbb{R}^2 \to \mathbb{R}^2$ with matrix $A = \begin{pmatrix} 1 & 1 \\ 1 & 2 \end{pmatrix} = \begin{pmatrix} 1 & 0 \\ 1 & 1 \end{pmatrix} \cdot \begin{pmatrix} 1 & 1 \\ 0 & 1 \end{pmatrix}$. Cutting and pasting appropriately the image parallelogram pattern we can check by hands that we can transform the new pattern to the initial square one.

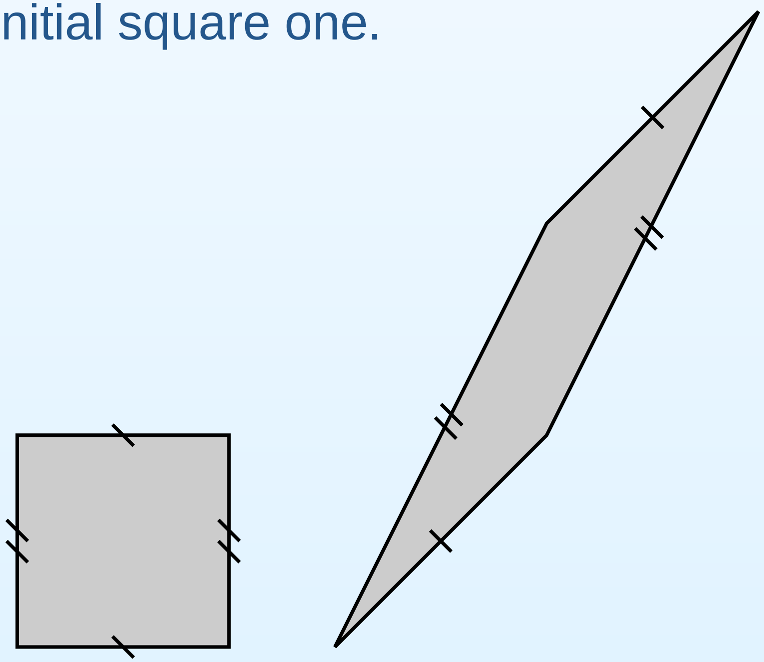

Pseudo-Anosov diffeomorphisms

Consider a composition of two Dehn twists $g = f_v \circ f_h =$

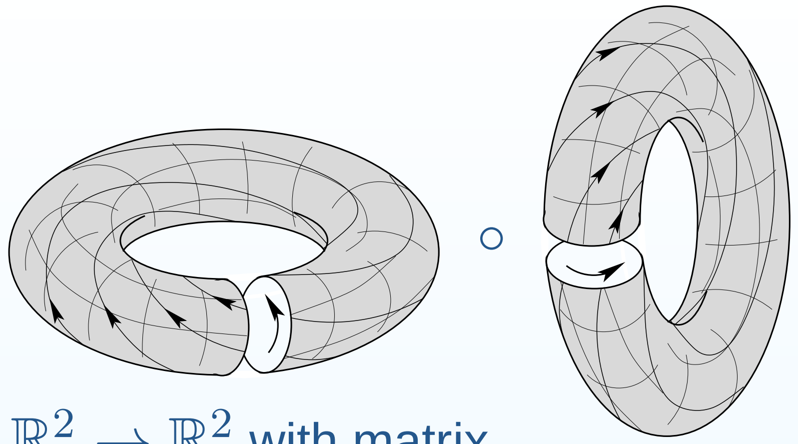

It corresponds to the integer linear map $\hat{g} : \mathbb{R}^2 \to \mathbb{R}^2$ with matrix $A = \begin{pmatrix} 1 & 1 \\ 1 & 2 \end{pmatrix} = \begin{pmatrix} 1 & 0 \\ 1 & 1 \end{pmatrix} \cdot \begin{pmatrix} 1 & 1 \\ 0 & 1 \end{pmatrix}$. Cutting and pasting appropriately the image parallelogram pattern we can check by hands that we can transform the new pattern to the initial square one.

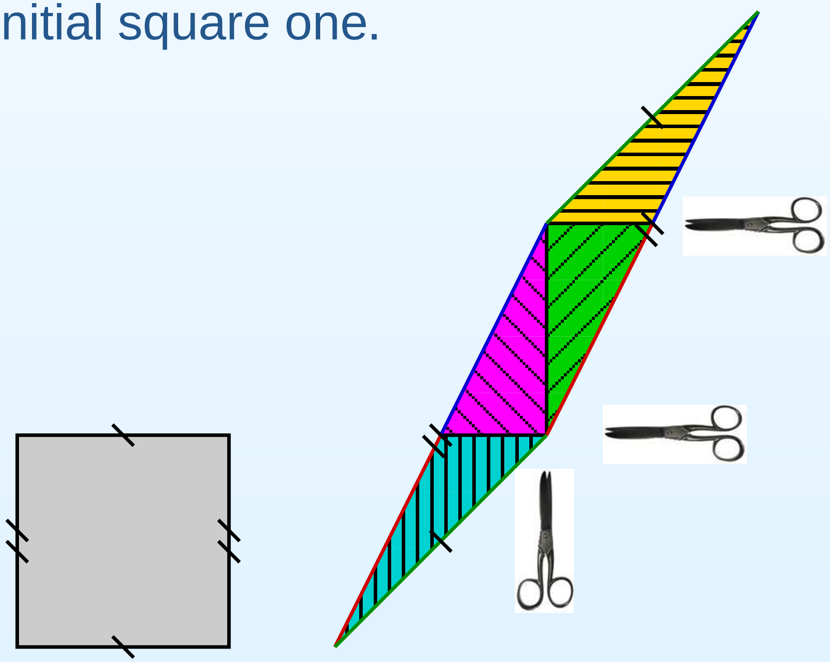

Pseudo-Anosov diffeomorphisms

Consider a composition of two Dehn twists $g = f_v \circ f_h =$ 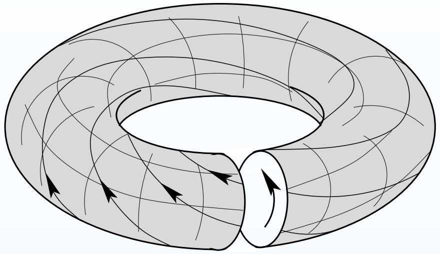 $\circ$ 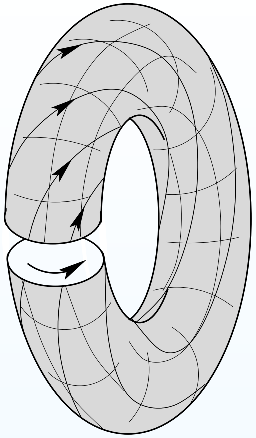

It corresponds to the integer linear map $\hat{g} : \mathbb{R}^2 \to \mathbb{R}^2$ with matrix $A = \begin{pmatrix} 1 & 1 \\ 1 & 2 \end{pmatrix} = \begin{pmatrix} 1 & 0 \\ 1 & 1 \end{pmatrix} \cdot \begin{pmatrix} 1 & 1 \\ 0 & 1 \end{pmatrix}$. Cutting and pasting appropriately the image parallelogram pattern we can check by hands that we can transform the new pattern to the initial square one.

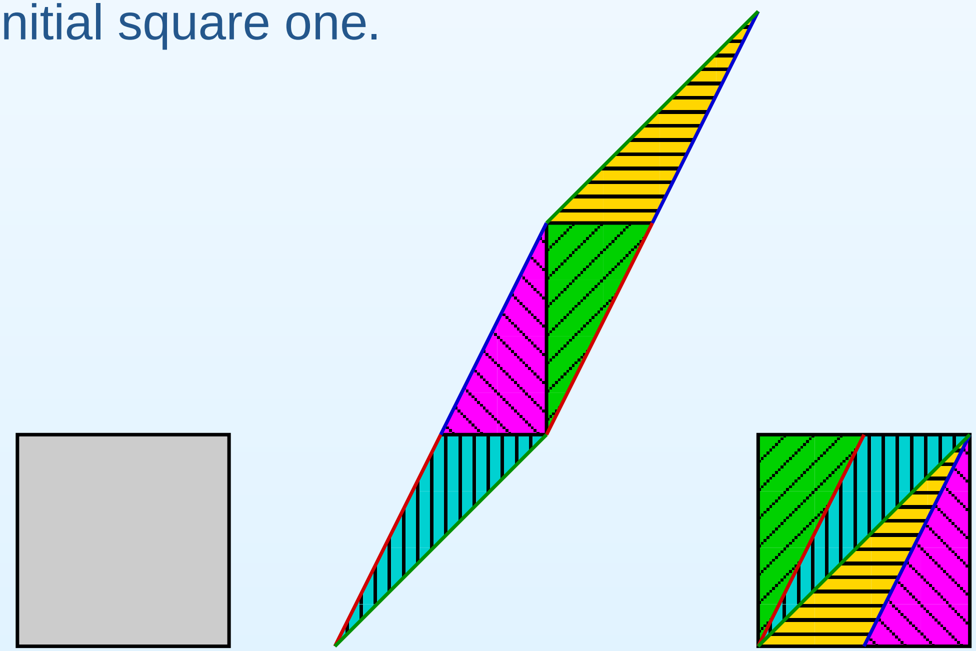

Closed geodesics in the space of tori

Consider eigenvectors $\vec{v}_{exp}$ and $\vec{v}_{contr}$ of the linear transformation $A = \begin{pmatrix} 1 & 1 \\ 1 & 2 \end{pmatrix}$ corresponding to the eigenvalues $\lambda > 1$ and to $1/\lambda < 1$ respectively. Consider two transversal foliations on the original torus in directions of $\vec{v}_{exp}$ and of $\vec{v}_{contr}$. We have just proved that expanding our torus $\mathbb{T}^2$ by factor λ in direction $\vec{v}_{exp}$ and contracting it by the factor λ in direction $\vec{v}_{contr}$ we get the original torus.

Closed geodesics in the space of tori

Consider eigenvectors $\vec{v}_{exp}$ and $\vec{v}_{contr}$ of the linear transformation $A = \begin{pmatrix} 1 & 1 \\ 1 & 2 \end{pmatrix}$ corresponding to the eigenvalues $\lambda > 1$ and to $1/\lambda < 1$ respectively. Consider two transversal foliations on the original torus in directions of $\vec{v}_{exp}$ and of $\vec{v}_{contr}$. We have just proved that expanding our torus $\mathbb{T}^2$ by factor λ in direction $\vec{v}_{exp}$ and contracting it by the factor λ in direction $\vec{v}_{contr}$ we get the original torus.

Consider a one-parameter family of flat tori obtained from the initial square torus by a continuous deformation expanding with a factor e^t in directions $\vec{v}_{exp}$ and contracting with a factor e^{-t} in direction $\vec{v}_{contr}$. By construction such one-parameter family defines a closed curve in the space of flat tori: after the time $t_0 = \log \lambda$ it closes up and follows itself.

One can check that this closed curve is, actually, a closed geodesics in the moduli spaces of tori.